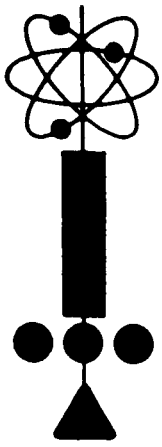

CONTRACT NO. NAS. 8-11423

DOCUMENT NO. 66SD2026

JULY 15, 1966

STUDY OF LOW ACCELERATION SPACE TRANSPORTATION SYSTEMS PHASE II STUDY REPORT

VOLUME I - SUMMARY

ADVANCED NUCLEAR SYSTEMS ENGINEERING

GENERAL ELECTRIC

MISSILE AND SPACE DIVISION

Valley Forge Space Technology Center

P.O. Box 8555 • Philadelphia 1, Penna.

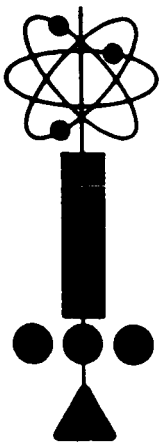

CONTRACT NO. NAS. 8-11423
DOCUMENT NO. 66SD2026
JULY 15, 1966

STUDY OF LOW ACCELERATION SPACE TRANSPORTATION SYSTEMS PHASE II STUDY REPORT

VOLUME I - SUMMARY

Prepared By: S L Coates
G. L. Coates, Study Program Manager

Prepared By: Harold Brown (TY)
H. Brown, Mgr., Mission Synthesis

ADVANCED NUCLEAR SYSTEMS ENGINEERING

GENERAL ELECTRIC
MISSILE AND SPACE DIVISION
Valley Forge Space Technology Center
P.O. Box 8555 • Philadelphia 1, Penna.

TABLE OF CONTENTS

LIST OF ILLUSTRATIONS

LIST OF ILLUSTRATIONS (CONT)

LIST OF TABLES

SECTION 1

INTRODUCTION

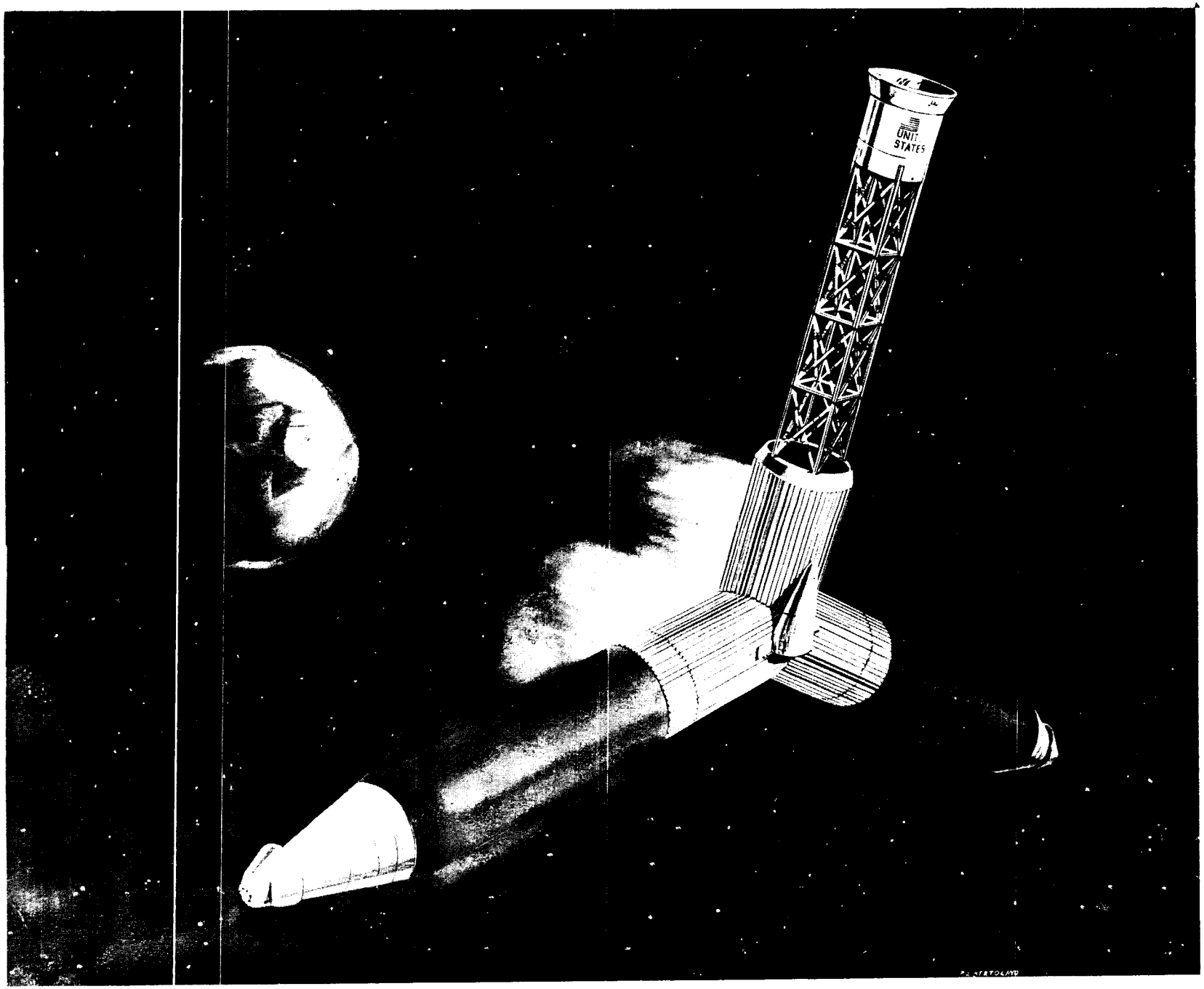

Eight Mw Manned Mars Vehicle

SECTION 1

INTRODUCTION

The Study of Low Acceleration Space Transportation Systems began in July 1964 with the objective of assessing the technical feasibility of using nuclear electric propulsion, assisted by nuclear rocket propulsion, for manned interplanetary travel. A 3 to 6 man landing on Mars (total crew: 6 to 12) was selected as the base line mission on which to focus the study. In July 1965 the contract was extended to further pursue this objective. Then in October 1965, the contract was expanded to consider solar-electric vehicles as well. Volume I of this report is a brief summary of the results obtained and conclusions drawn to date. Volume II has the same organization as Volume I, covering the same ground in much more detail and including several minor topics which were omitted from the Summary.

The reference mission profile is shown in Figure 1. The vehicle is assumed to be assembled in a low Earth orbit. It departs from that orbit via a nuclear rocket Earth departure stage which provides it with an optimum hyperbolic velocity relative to the Earth. The electric propulsion then takes over, operating for a few months to place the vehicle on the proper heliocentric coast trajectory. Following a few months of coast, the electric propulsion is restarted to carry the vehicle into rendezvous with Mars and thence through a spiral descent to a final circular orbit. The Mars excursion module then separates and lands part of the crew on the surface for 40 days of exploration. This module then returns the crew to the main spaceship and is subsequently abandoned. Electric propulsion is used to spiral the vehicle out to Mars escape and then to place it on the proper inbound coast trajectory. Following several months of coasting the electric propulsion is started for the fourth time to bring the vehicle into rendezvous with Earth and finally into a high orbit around Earth, where the crew is retrieved by a landing vehicle launched from the surface.

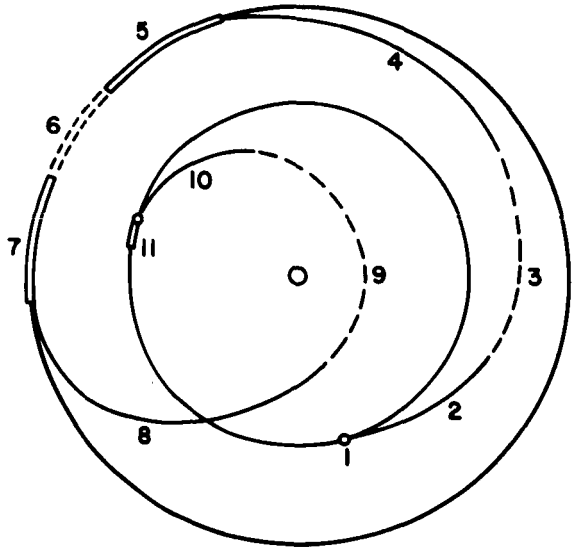

EVENT	PROPULSION	DESCRIPTION
1	NU. ROCKET	HYP. EARTH ESCAPE
2	ELECTRIC	OUTBOUND TRANSFER
3	NONE	OUTBOUND COAST
4	ELECTRIC	RENDEZVOUS WITH MARS
5	ELECTRIC	MARS DESCENT
6	NONE	MARS EXPLORATION
7	ELECTRIC	MARS ESCAPE
8	ELECTRIC	INBOUND TRANSFER
9	NONE	INBOUND COAST
10	ELECTRIC	RENDEZVOUS WITH EARTH
11	ELECTRIC	EARTH CAPTURE

Figure 1. Mission Profile

Several variations in this profile are under consideration. First, it is possible to end the mission with the main spacecraft flying past the Earth and the crew making a direct hyperbolic velocity entry into the Earth's atmosphere in a specially constructed entry module. This greatly reduces the propulsion requirements and, hence, either the initial gross weight of the spaceship or the trip time. It eliminates the fourth electric propulsion phase entirely and thus greatly reduces the lifetime required of the powerplant and propulsion system. These advantages are faced by several operational disadvantages; however, in balance the mode looks very attractive. A second variation is the possible use of high thrust propulsion for Mars capture and/or departure. This option is still under study.

The study has touched on all of the technical areas involved in the mission which were expected to have a first order effect on its technical feasibility; the results in each of these areas are discussed in Sections 2 through 9 below. Section 10 is a brief statement of the conclusions drawn to date.

SECTION 2

MISSION ANALYSIS TECHNIQUES

The ability to calculate vehicle performance, and the ability to rapidly determine the particular set of vehicle and trajectory characteristics which will maximixe that performance, is a prerequisite to any feasibility study of this type. The approach used in this study may be summarized as follows:

1. Assemble a matrix of low thrust propulsion requirements from explicit optimum trajectory calculations.

2. Fit the above data with empirical equations (a "trajectory model") which will permit calculation of the performance of a particular vehicle/trajectory combination in milliseconds.

3. Combine the trajectory model with design-based vehicle subsystem models and with a multivariable optimization routine to calculate (in 2 or 3 minutes) an optimum vehicle/trajectory combination for the mission at hand. (Note that such an optimization includes 200 to 400 calculations of performance. The use of an explicit trajectory calculation for each of these would be prohibitively expensive; hence, the empirical trajectory modeling approach.)

The reference matrix of trajectory data has consisted so far of trajectories calculated by JPL and of additional cases run by GE using the JPL computer program. Now, however, the nuclear-electric vehicle studies have progressed to the point where new data are needed. The required data showing the effects of hyperbolic approach to or departure from Mars could be generated by the JPL program, but this would be a time-consuming task. Data showing the effects of the expected declining power characteristics of real power plants and propulsion systems cannot be generated by this means.

Expansion of the study to include solar-electric vehicles also meant a requirement for solar-electric trajectories which could not be calculated by existing computer programs. GE has, therefore, developed a trajectory program tailored to this need. The program can calculate optimum heliocentric trajectories under any imposed power profile for either the optimum variable or the constant specific impulse mode of operation. The precision of the present program is sufficient for the performance part of a feasibility study; future development is expected to enhance the precision to the point where it can be used to generate precise histories of, for example, thrust vector magnitude and direction. The program is also potentially extendable to include the 3 body planeto-centric to heliocentric transition regions. The unique approach used in this trajectory program is described in Volume II.

The mission model used in the overall vehicle/trajectory optimization is shown in Figure 2. The input is divided into two categories; variables to be optimized and parameters which are fixed on any one run but which can be systematically varied in

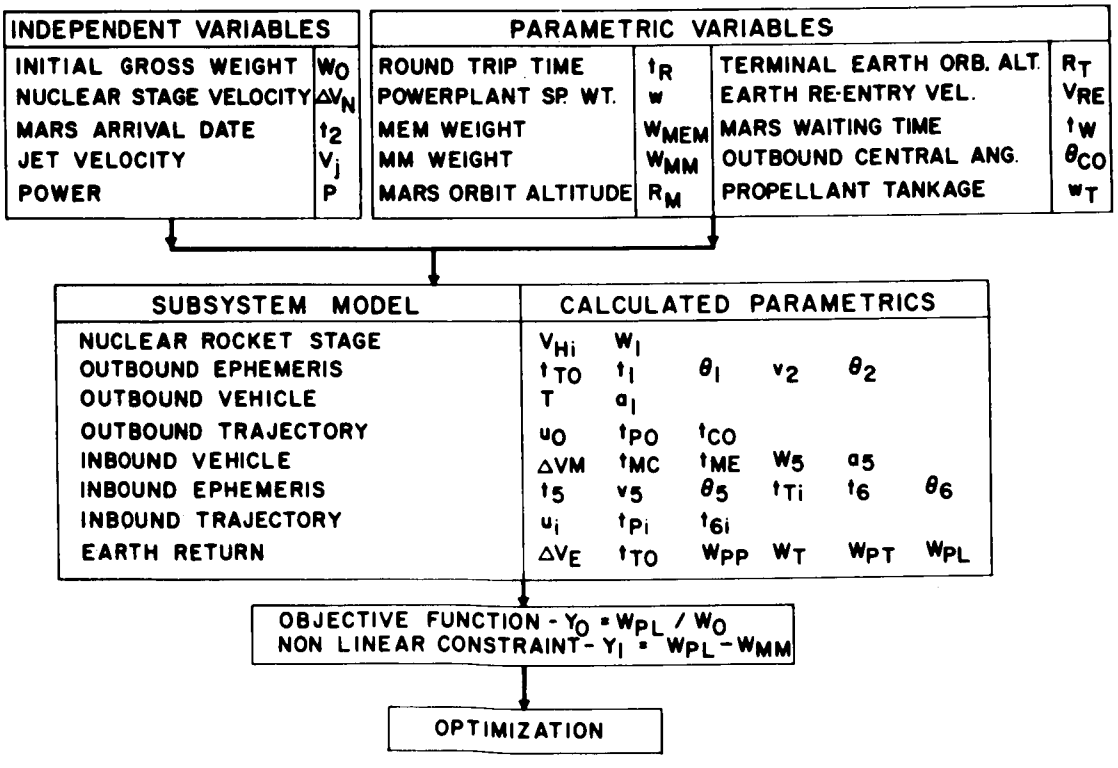

Figure 2. Manned Mars Mission Model

I

a series of runs. The division shown is not rigid; variables can be readily moved from one category to another provided that this does not destroy the existence of a real optimum solution. The optimization criterion used (by NASA direction) is that of minimum initial mass in Earth orbit for a given payload. However, this could readily be changed should another criterion prove more desirable.

SECTION 3

PAYLOAD MODULES

The nominal mission module configuration is illustrated in Figure 3. The central feature is a combined command-and-control center and solar flare shelter, which is surrounded by living quarters, work area, and recreation facilities. The sketch indicates a very thick solar flare shield based upon an early assumption. The thickness of this shield has since been greatly reduced, as discussed in detail in Volume II.

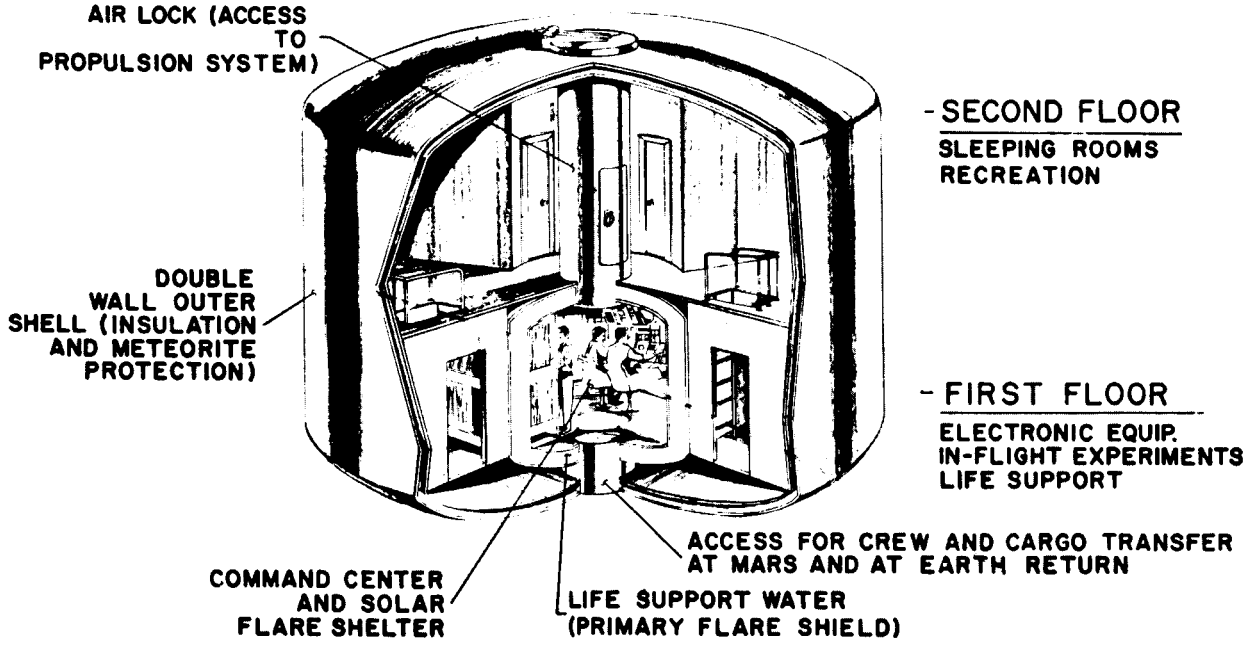

Figure 3. Nominal Mission Module

A generous gross inside volume of 40 m^3 (~1400 ft^3) per man is provided by the module. A semi-closed life support system is assumed which provides 95% water recovery for reuse, but does not recover oxygen from the CO_2 produced in the air.

Figure 4 shows some typical module weights calculated from these assumptions as detailed in Volume II.

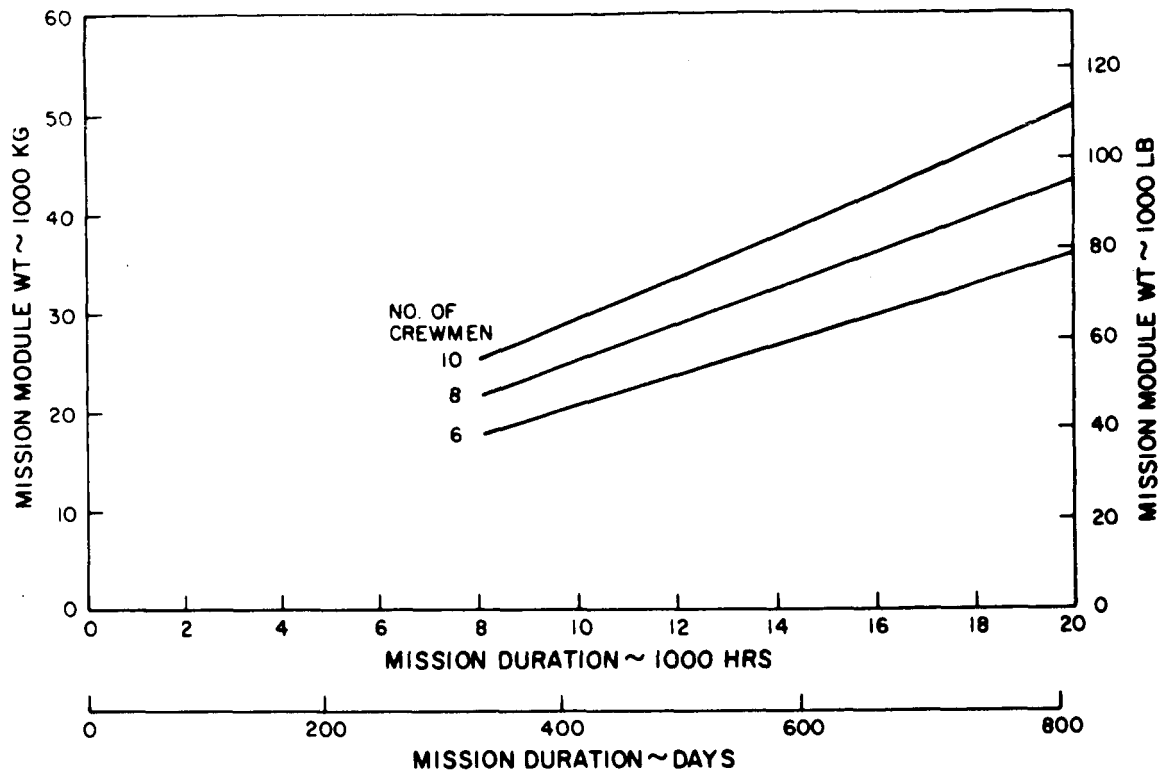

Figure 4. Mission Module Weights

A lifting body Mars excursion module has been assumed as shown in Figure 5. A number of entry trajectories were calculated to explore the design implications of the Mariner IV Mars atmosphere data. Figure 6 shows one major result; the Mars landing footprint is markedly lengthened and narrowed but remains essentially unchanged in area. Other calculations, described in Volume II, have shown that although the new atmosphere rearranges the design of the module, its gross weight is not significantly changed.

Approximate scaling factors were used to estimate the variation of the Mars excursion module weight with the main spaceship orbit altitude. The results, shown in Figure 7, were used as input to studies (described in Section 9) of the effect of Mars orbit

I

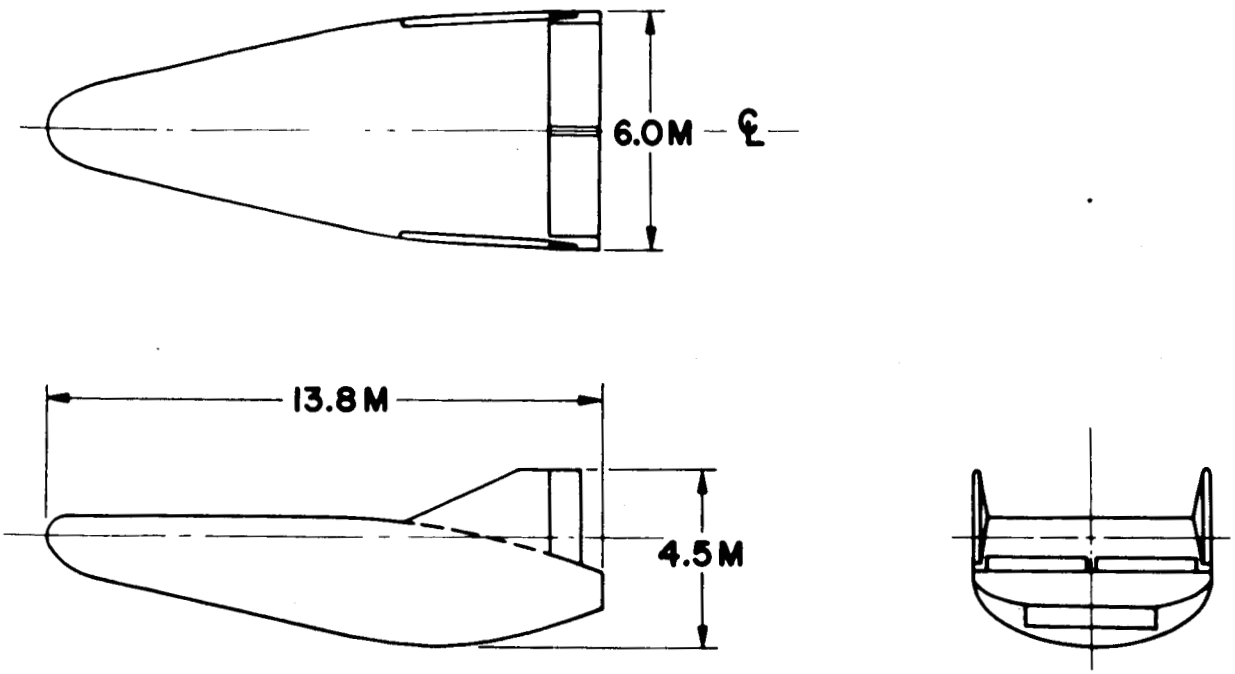

Figure 5. Mars Excursion Module (Basic Configuration M-2, F-2)

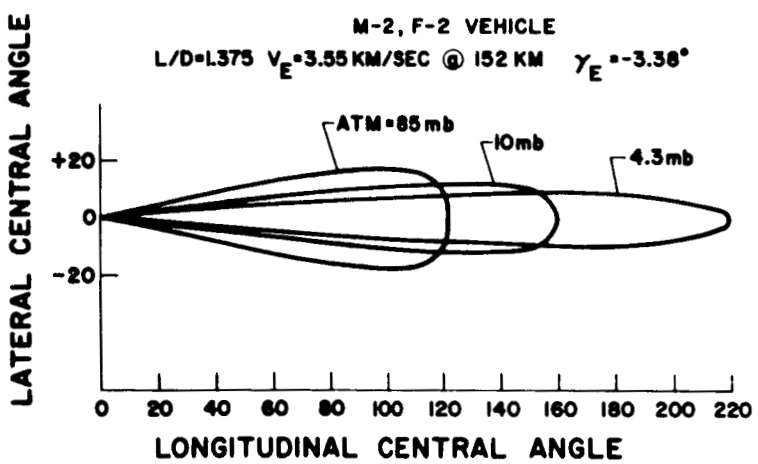

Figure 6. Effect of Atmosphere Model on Landing Footprint

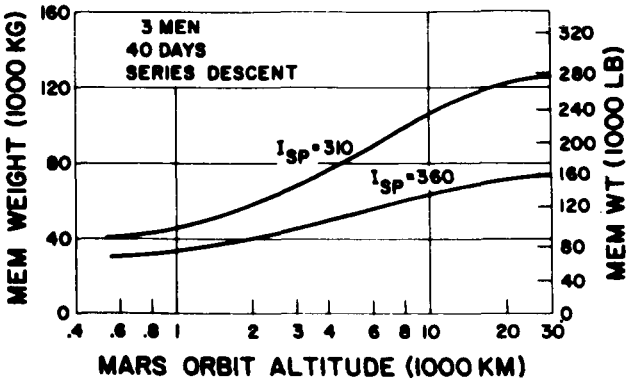

Figure 7. Typical Mars Excursion Module Weights

altitude on the overall spaceship size and power. Figure 7 also shows the major differences in Mars excursion module weight resulting from the differences between present day operational storable propellants (I_{sp} = 310) and the more advanced propellants currently being tested (I_{sp} = 360).

SECTION 4

PROPULSION SYSTEMS

Three different principle types of propulsion may be involved in conveying a manned vehicle from the Earth assembly orbit through an interplanetary mission. These propulsion systems (the main electric propulsion, the nuclear rocket Earth departure stage, and the high thrust units used at Mars) are discussed below.

4.1 ELECTRIC PROPULSION

The study to date has assumed the use of electrostatic ion thrustors simply because their characteristics are relatively well understood at this time. Should any of the several promising competitors eventually prove superior, the vehicle performance can be happily upgraded.

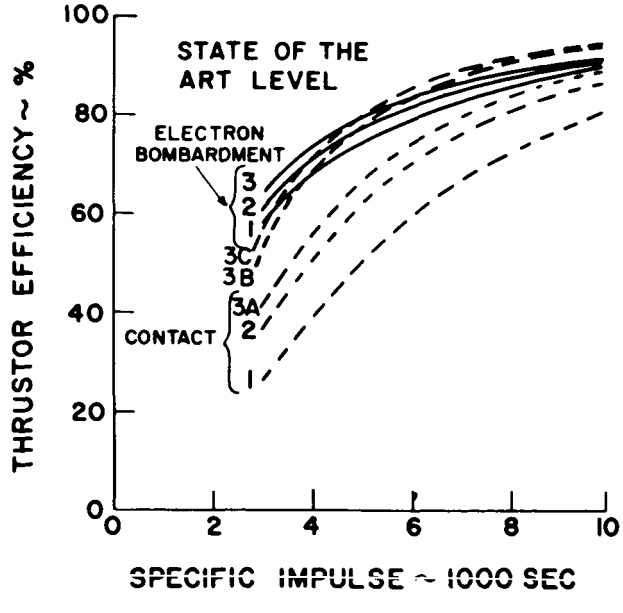

Figure 8. Thrustor Efficiency

Figure 8 and 9 show the thrustor efficiencies, sizes and weights estimated for mercury electron bombardment and cesium contact ion thrustors at various state-of-the-art levels. At the time the data was generated (December 1964) the contact engine levels 1, 2, and 3A were intended to be roughly comparable to the electron bombardment levels 1, 2, and 3. As one would expect, a great deal has happened in thrustor technology since then and the whole subject is now up for review, particularly

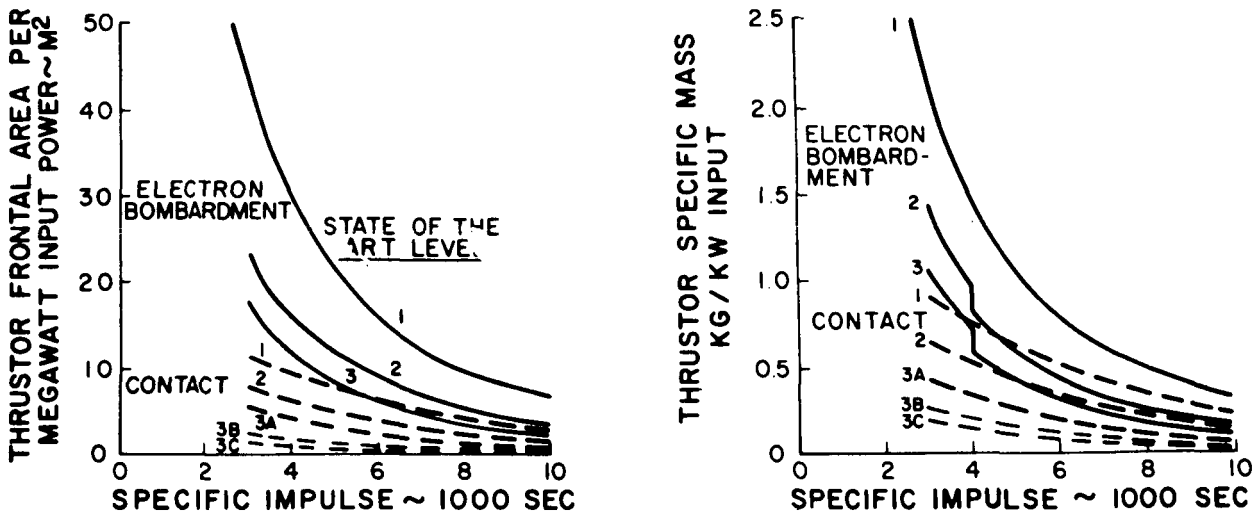

Figure 9. Thrustor Size and Weight

the relative levels of the two thrustor types. Nearly all of the vehicle performance work to date has assumed the use of the level 2 electron bombardment thrustor, and its characteristics are still regarded as representative of a 1975 ion thrustor rated for a long life (e.g., 10,000 hours) and high reliability (e.g., 0.98).

Each vehicle performance point presented in this report results from a simultaneous optimization of ion thrustor specific impulse, power, Earth departure stage size, outboard trip time and Mars arrival date. The optimum Isp values have ranged from 4500 to 6500 seconds depending on trip time, powerplant specific weight, and thrustor selection.

Figure 10 is a simplified schematic of the electric propulsion power conditioning, switching and control system. Its weight is estimated to be 1.06 kg/kw without redundancy and without the auxilliary cooling system. Redundancy provisions may increase the weight by 30% or so depending on the specific case. The auxilliary cooling system is a significant item which has not been explicity studied so far; its weight is largely accounted for, however, in that the weight of a complete, strong propulsion system outer shell is included in the overall system weight and the auxilliary radiators would merely replace sections of this outer shell. The power conditioning efficiency is estimated to be 96% for these advanced systems.

A series of design studies of complete electric propulsion systems integrated into overall vehicle designs has led to the following expression for the electric propulsion system weight

$$W = (K_1 K_2 W_{st} + W_{spc}) P + (1 + K_3) W_P$$

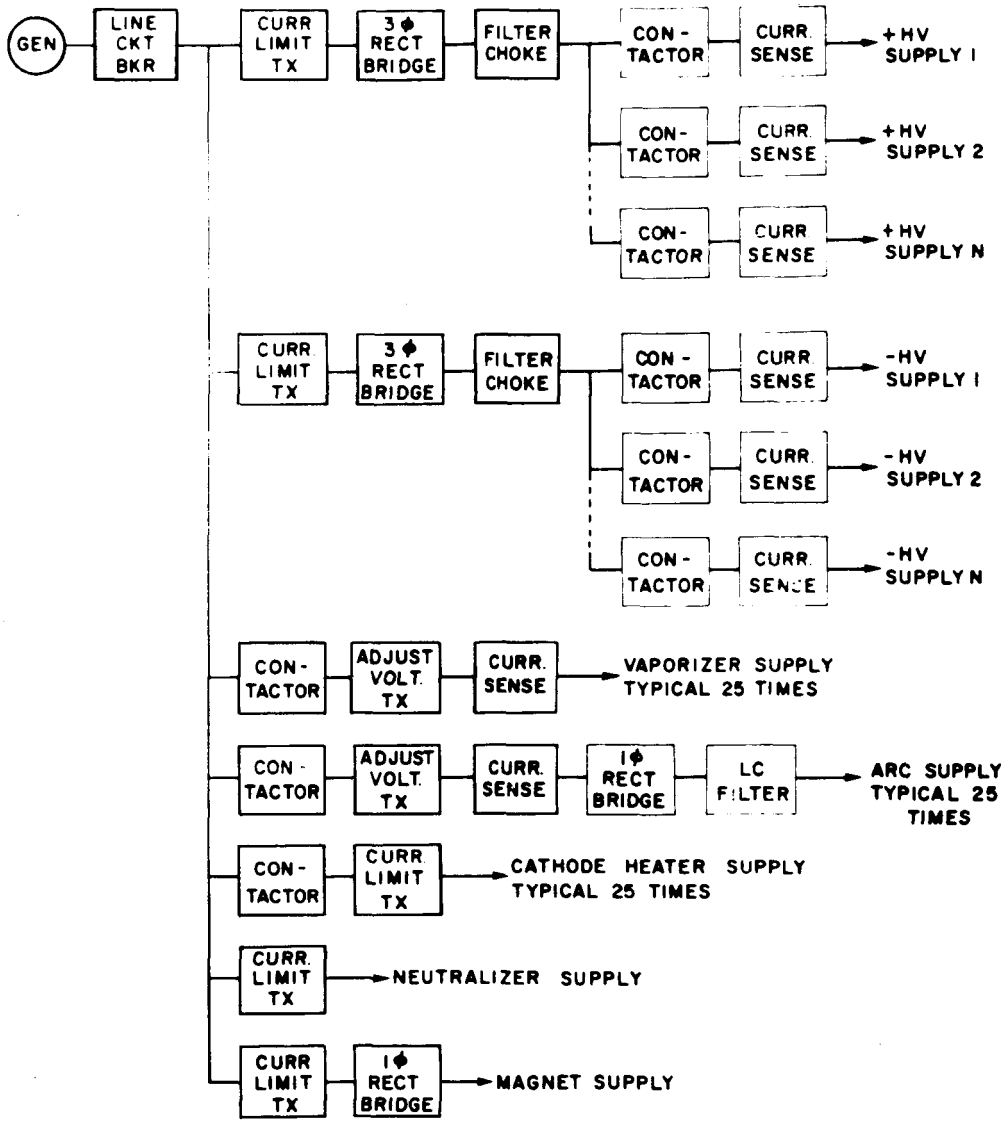

Figure 10. Power Conditioning Schematic

K_1 = Thrustor redundancy factor

K_2 = Thrustor support structure factor

= 1.1 for fixed circular arrays

= 1.4 for rectangular arrays

K_3 = Tankage structure factor

= .065 for cesium in fixed arrays

= .03 for mercury in fixed arrays

= .10 for deployable arrays

P = Power supplied to propulsion system

W_P = Propellant weight

W_{st} = Individual thrustor specific weight (Figure 9)

W_{spc} = PCSC specific weight including reliability factors (assumed to be 1.9 kg/kwe in the work to date)

4.2 DIRECTLY HEATED IONIZERS

A conceptual design study of the idea of improving efficiency by transfering heat directly from the reactor to the ionizers of contact thrustors (rather than converting reactor heat to electricity and then electrically heating the ionizers) has revealed that this may improve the overall system specific weight provided that the turbomachinery for generating the rest of the electrical power is designed to take advantage of the ~ 1560°K (2270°F) required average reactor outlet temperature. This implies a turbine inlet temperature of perhaps 1477°K (2200°F) which is definitely stretching the technology. With a more realistic 1284°K (1850°F) turbine inlet temperature the directly heated ionizer system shows no specific weight advantage, leaving it with only the disadvantage of a reactor temperature some 224°K (325°F) higher than would otherwise be required.

4.3 EARTH DEPARTURE STAGE

A single Nerva II nuclear rocket engine having a thrust of 1,100,000 N (250,000 lb), a specific impulse of 800 seconds, and a weight of 13,900 kg (30,600 lb) has been

assumed for the Earth departure stage in the work to date. The stage structural weight has been assumed (on the basis of a conceptual design layout) to be 11.4% of the propellant weight. Recent results of the Nerva tests have generated confidence that a specific impulse of 850 seconds is a reasonable design objective, and it is recommended that this value be used in future work. At the same time a standard nuclear rocket stage module concept has evolved at MSFC in which some stage structural weight penalties are accepted in the interests of standardization and operational simplicity. The use of these modules should also be assumed in future work.

4.4 HIGH THRUST PROPULSION AT MARS

The very preliminary investigations conducted here of the implications of high thrust propulsion at Mars have assumed that separate stages would be used for capture and departure and that the Earth departure weight of each stage could be represented by:

$$W = A + (1 + B + C)\, W_P$$

where A is the engine and thrust structure weight, B is the thermo-meteoroid protection system mass fraction (assumed to be jettisioned at engine startup), C is the tankage mass fraction, and W_P is the propellant weight. The following numerical values were used.

Item	Nuclear Stage	Chemical Stage
A	14000 kg	2700 kg
B	7%	0
C	13%	5%

These data were extracted from other previous work, and do not reflect the vehicle integration aspects of the problem which will almost certainly be prominant in this application. Hence, they are up for design study in the coming months.

SECTION 5

NUCLEAR POWERPLANT

A 4-loop Rankine cycle powerplant concept is the base line for all of the nuclear-electric vehicle studies under this contract. A schematic drawing of such a powerplant is shown in Figure 11. The lithium primary loop carries heat from the reactor to a heat exchanger located in the shield near the reactor. The lithium secondary loop carries the heat to the boilers in a parallel set of 4 independent power conversion units. Each of these units contains a complete boiler-turbine-condenser potassium power conversion loop. The fourth "loop" (actually 4 loops in parallel) then rejects the waste heat through the primary radiator. Auxilliary cooling loops are also provided as indicated.

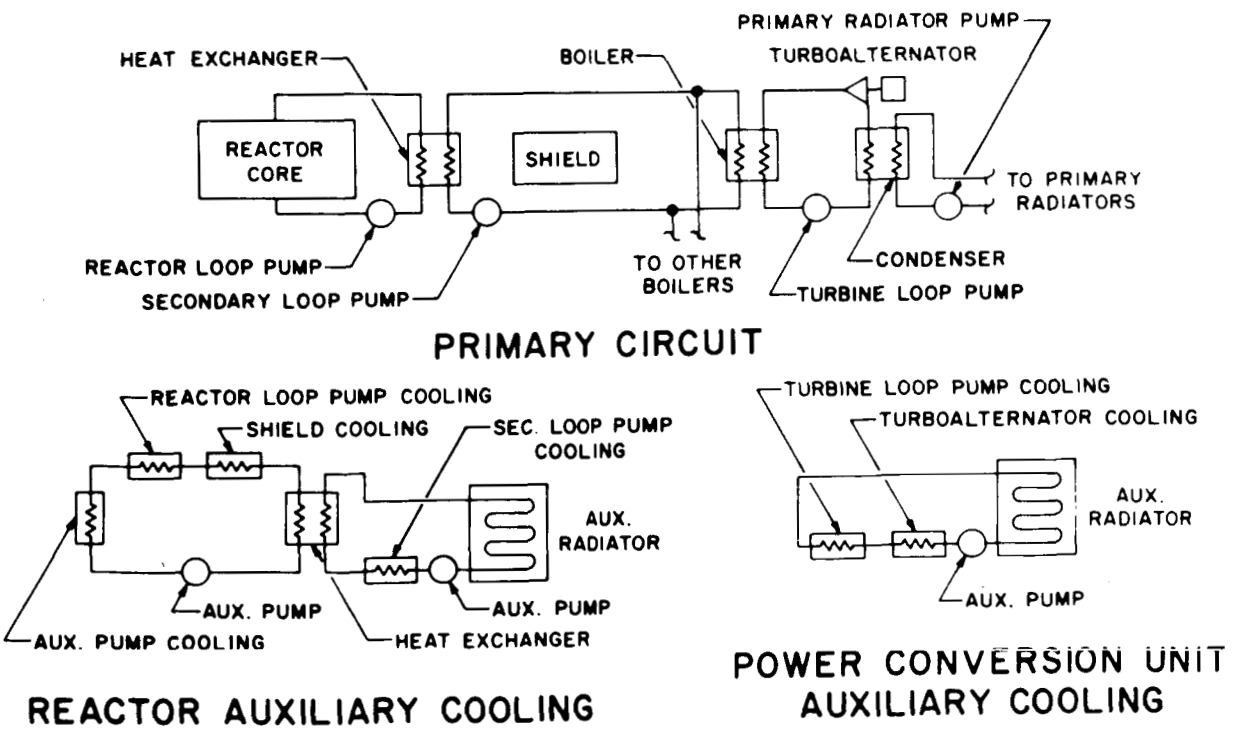

Figure 11. Powerplant Schematics

Volume II details the shielding analyses conducted for both the single powerplant and dual powerplant vehicle configurations. The dual powerplant task, described in Figure 12, is the most complex and has been given the most complete analysis. The shield design evolved for this situation is shown in Figure 13. Note that the heat exchanger which joins the primary and secondary loops is located so as to have heavy shielding between it and the crew, thus eliminating radiation hazards due to primary loop activation and fission fragment release into the primary loop. It also has some shielding between it and the reactor to prevent secondary loop activation. The weight of the complete reactor assembly (reactor, shield, controls, pumps, plumbing and auxilliary cooling system) is shown as a function of energy output, fuel burnup, power, and radiator cone angle (i.e., scatter shield cone angle) in Figure 14. The weights are observed to be very high due to the side lobes of shielding needed to separately protect the mission module and the other powerplant. A single powerplant vehicle

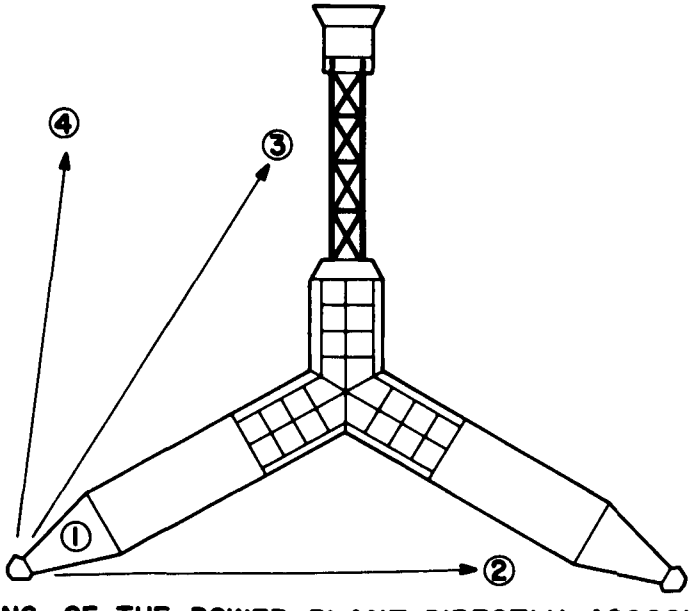

(1) SCATTER SHIELDING OF THE POWER PLANT DIRECTLY ASSOCIATED WITH THE REACTOR
(2) SCATTER SHIELDING OF THE OTHER POWER PLANT
(3) SHADOW SHIELDING OF THE MISSION MODULE
(4) SHADOW SHIELDING OF THE MEM DEPARTURE AND RETURN CORRIDOR

Figure 12. Shielding Requirement

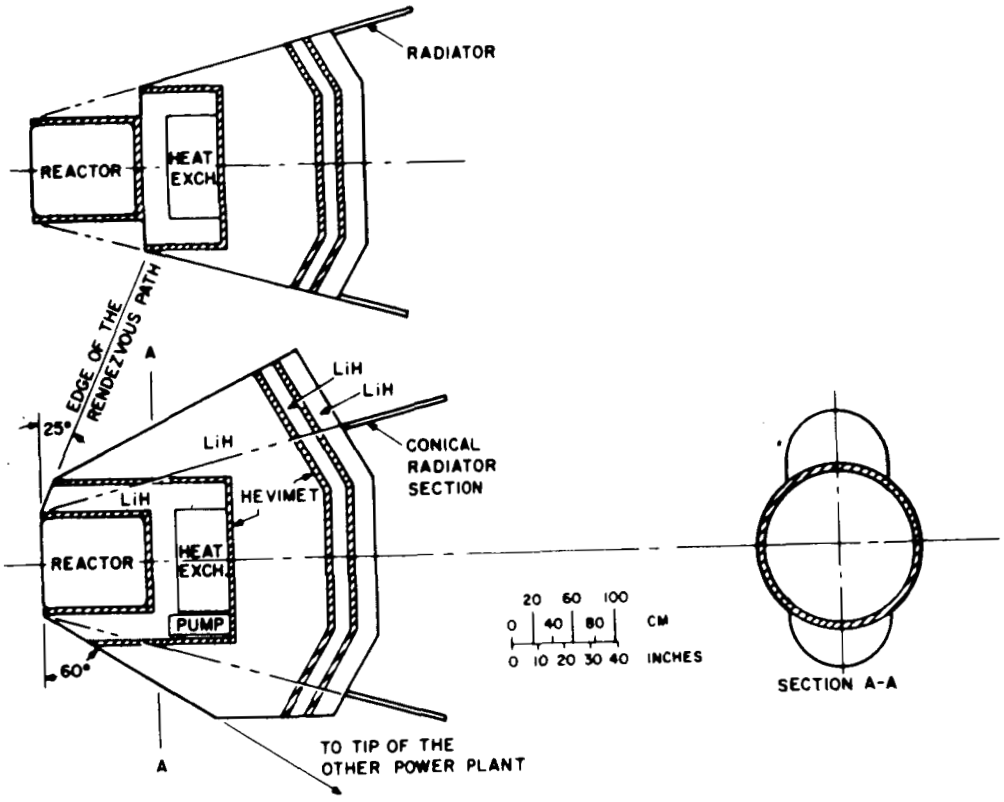

Figure 13. Shield Concept

configuration would reduce these weights by up to 40%. The pronounced effect of cone angle is characteristic of both single and dual powerplant designs. Large powerplants are usually limited in radiator area by launch vehicle payload envelope limits; this tends to drive the cone angle up and an optimum compromize must be sought. This situation argues for the development of ways to extend or circuvent the launch envelope constraint.

Reliability studies have led to the tentative selection of a powerplant concept in which each of 4 power conversion units has a 33% reserve capacity so that any 3 of the 4 can provide full powerplant output. These studies have also led to the assumed use of electromagnetic rather than motor pumps throughout the system. A series of power-plant efficiency calculations on this basis led to the data shown in Figure 15.

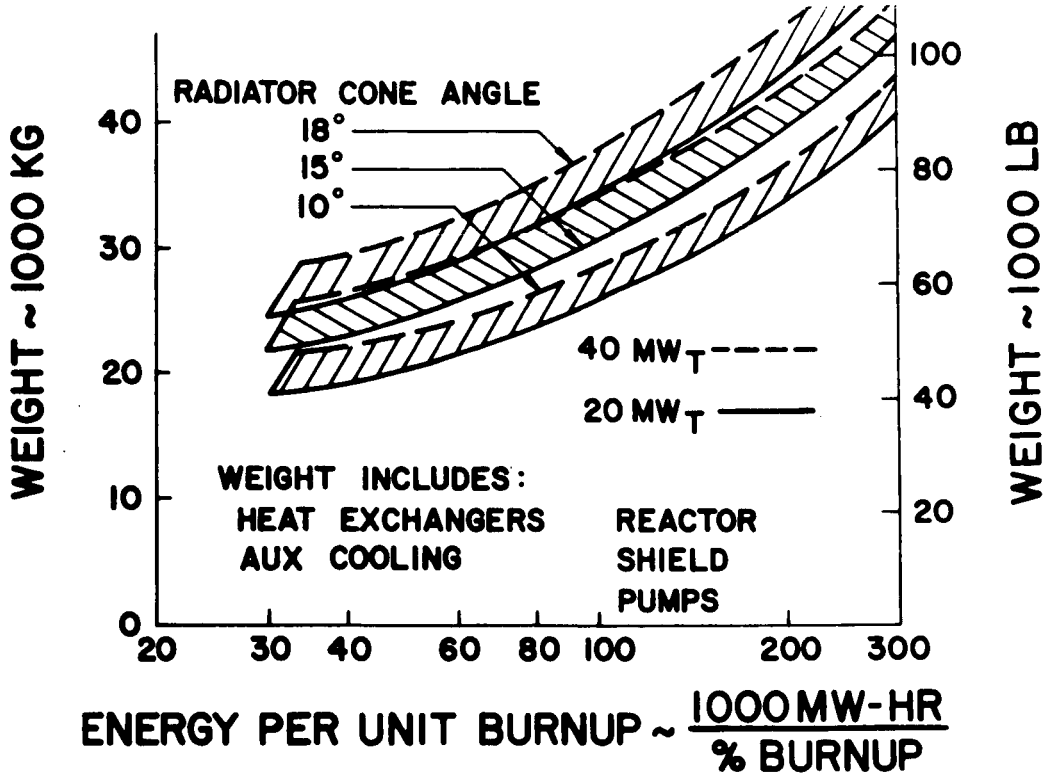

Figure 14. Reactor and Shield Assembly Weight

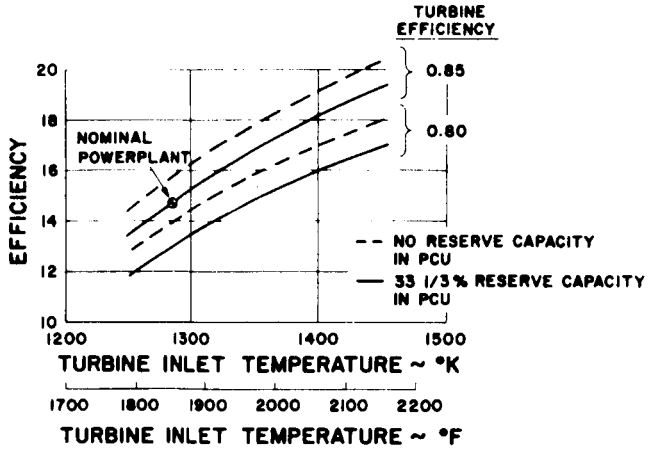

Figure 15. Overall Power Conversion Efficiency

A review of the status of Rankine powerplant technology indicated that the future development of this technology might logically follow the sequence shown in Figure 16. The overall powerplant performance and specific weight was calculated for 18° cone angle 4 Mw powerplants with dual powerplant shielding at each state-of-the-art level; the results are also shown in Figure 16. It is observed that most of the

performance gain is achieved by level 3, and so this level is chosen as the base line technology for this study. The use of a single powerplant vehicle concept without radiator area limits could lower these specific weights by 30% or so; however the selection of level 3 would not be affected.

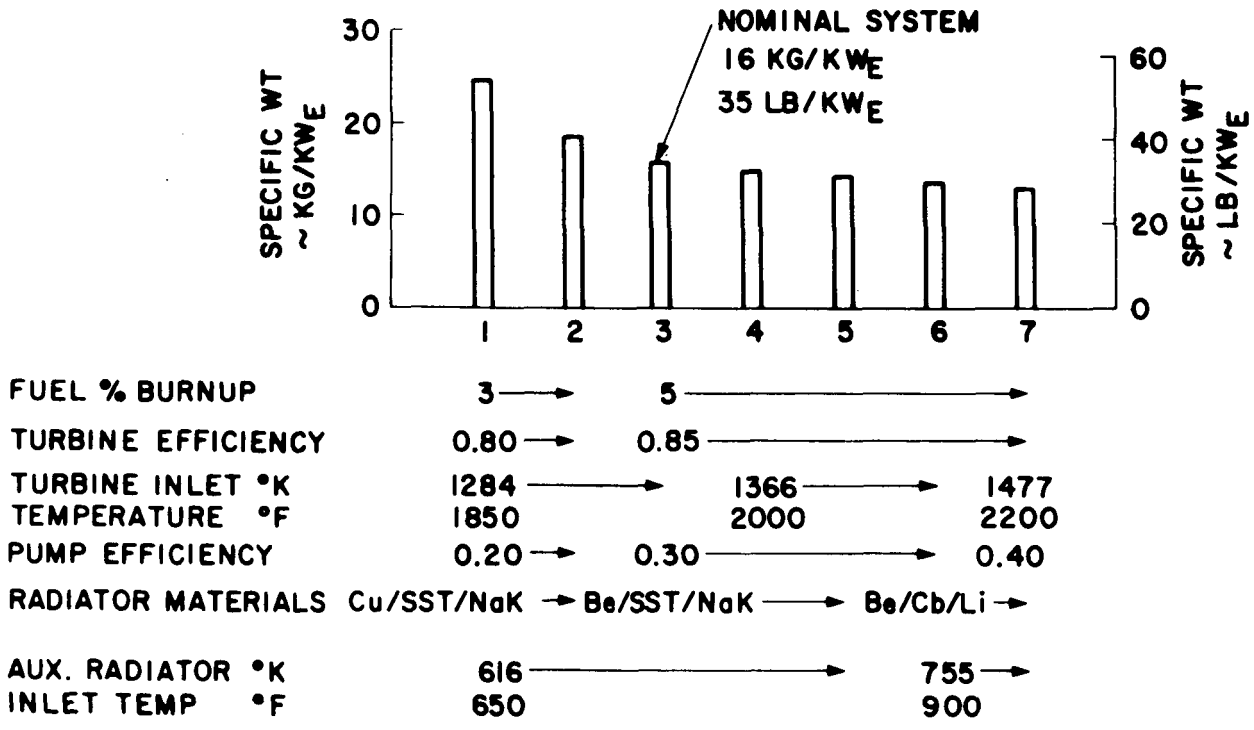

Figure 16. Powerplant State of the Art Levels

SECTION 6

RELIABILITY

The first fact one faces in considering the reliability of advanced systems is the total absence of basic reliability data on the components involved. In this situation, one cannot pretend to predict system reliability with any confidence at all. One can, however, establish methods of reliability prediction and use them to identify reliability goals for the components, design objectives which, if realized, would produce the desired system reliability. Further, these methods can be used to explore the effects of the various reliability improvement stratagems which can be used. The product, then, consists of the identification of critical components, a reasonable set of preliminary component reliability objectives, a plausible overall reliability strategy, and a first cut at the system performance penalties associated with establishing a man-rated level of reliability. This section presents the initial results of such an investigation.

The four stratagems which are available for use in providing the required high probability of safe crew return from a manned interplanetary mission are as follows:

- Increase component reliability through more intensive development and testing.
- Use component derating, redundancy, maintenance and repair to increase the probability of full power throughout the mission.
- Plan the mission for a declining power capability.
- Accept a modest reliability for following the nominal trajectory and provide a high reliability abort capability.

These stratagems are not at all new; they have all been in use for years. The question is: which procedure, or combination of procedures, best meets the needs of a manned

nuclear electric vehicle? It is fairly easy to show that no one stratagem will suffice; any one used alone leads to absurdly high costs and/or vehicle size requirements. A combination of stratagems, however, can achieve the required reliability at a reasonable cost, as shown below.

The problems of providing high reliability in the crew compartment (communications, guidance, life support, etc.) and in the high thrust stages have been treated elsewhere, hence attention is concentrated here on the nuclear powerplant and the electric propulsion system.

The general assumptions made in this preliminary attack on the problem are as follows:

1. All components have constant failure rate characteristics.
2. Each component is either operable at any power up to full power, or has failed completely.
3. Redundant failure sensing assures that all significant failures will be detected.
4. The crew can verify the indicated failures and, through manual backup, assure successful switching to standby units.
5. The powerplant operates continuously until either failure or mission end.
6. The propulsion operating time is 80 percent of the flight time.

The first two assumptions are standard for first cut investigations for two reasons; they greatly simplify the mathematics and they are reasonably good for most components. In the case at hand, they are expected to apply very well to many components, such as the radiator segments, but to have questionable validity for components such as the reactor core. Assumptions three and four are expected to be quite valid for the large 1985-model manned vehicle under consideration here. The vehicle provides plenty of space for easy access packaging and, in most cases, the switchover to a standby unit can, if necessary, be delayed for hours without significantly impairing the mission.

The question of what to do with the nuclear powerplant during coast periods has not yet been resolved. Continuous operation obviously means wasted power and a significant penalty in reactor size and shield weight. However, the shutdown and restart operations are complex (a reliability problem) and add technical problems (e.g., freezing of liquid metal coolants). Continuous operation may well turn out to be the best procedure and, since it simplifies the analysis, it is assumed here. The final assumption is an obvious simplification whose effect is small compared to the possible variations in component failure rates.

The reliability study has centered on the dual powerplant vehicle design. Preliminary investigations documented in Volume II led to a configuration in which each powerplant was assumed to consist of the components shown in Figure 17. The system divides first into a reactor assembly, four independent power conversion units, and at least 24 independent primary radiator segments. Within the reactor assembly, 100 percent

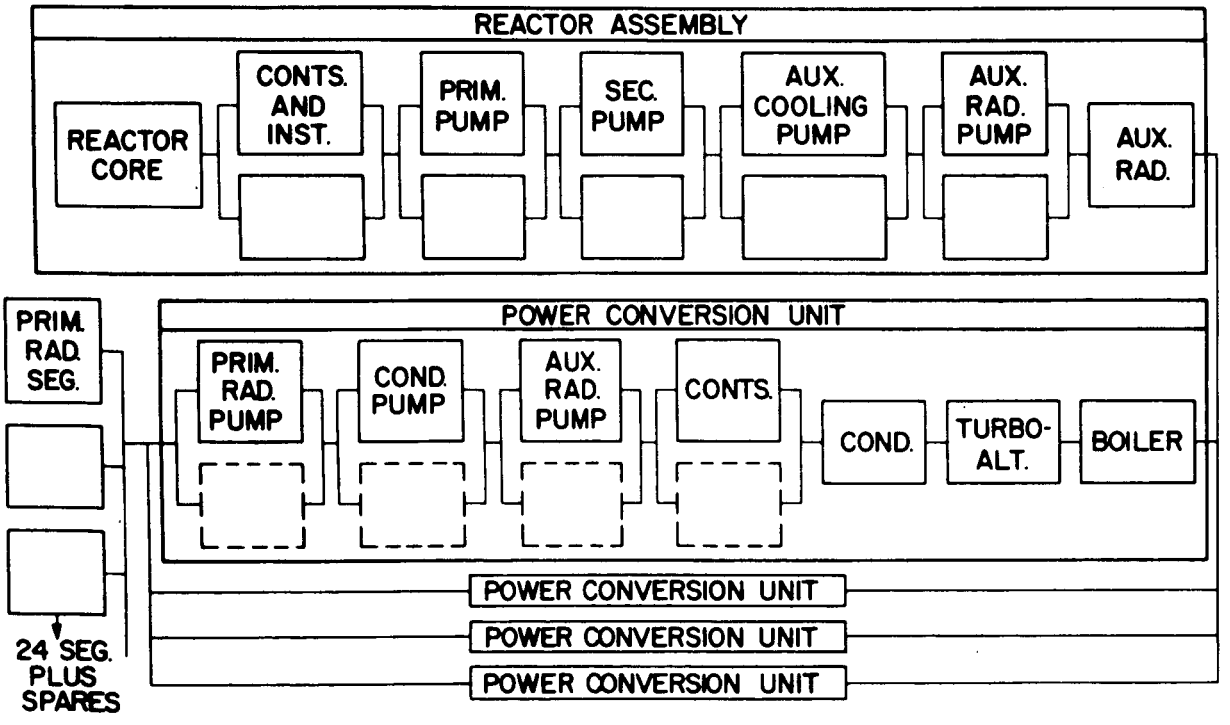

Figure 17. Powerplant Reliability Schematic

redundancy can be provided for the controls and for all pumps. The two pumps comprising each redundant pair are physically in series so that no valves are required; the switchover from one to the other involves only the electrical power. The pumps are in parallel from the viewpoint of reliability calculations, and hence are shown this way in the figure. Each power conversion unit is assumed to be designed to deliver 1/3 of the powerplant output; hence, any 3 of the 4 can deliver the full power output. Normal operation consists of running all four units (at 3/4 rated power each) until one fails, whereupon the remaining 3 move up to capacity output. It is readily feasible to provide redundant controls and pumps within each power conversion unit as indicated by the dashed lines. The number of spares to be provided is a parameter in the analysis below. Each primary radiator segment is sized for 1/24th of the total primary heat rejection; thus, at least 24 segments are provided. The number of additional, spare segments to be provided is also a parameter in the analysis below. It is assumed that the segments can be shut off individually in the event of a meteoroid puncture and that they are interconnected such that any segment can serve any power conversion unit within that powerplant.

Eight sets of transmission lines carry the electrical power from the eight turboalternators in the two powerplants to the electric propulsion system. This system is assumed to be divided into 24 independent propulsion modules. Switchgear is provided, in a central power distribution system, to assign specific propulsion modules to specific turboalternators. This provides complete flexibility in adapting to various combinations of failures and permits the turboalternators to operate independently, avoiding the need for synchronizing their outputs. As shown in Figure 18, each propulsion module contains a group of thrustors and a complete power conditioning, switching and control (PCSC) system. The PCSC system is broken down for analysis into 3 kinds of units; the transformer for the beam current power supply; a block of equipment which serves the modules as a whole; and additional blocks of equipment each of which serves an individual thrustor. It is arbitrarily assumed that each module contains 7 operating thrustors plus a variable number of spare thrustors (each thrustor having its own thrustor PCSC set).

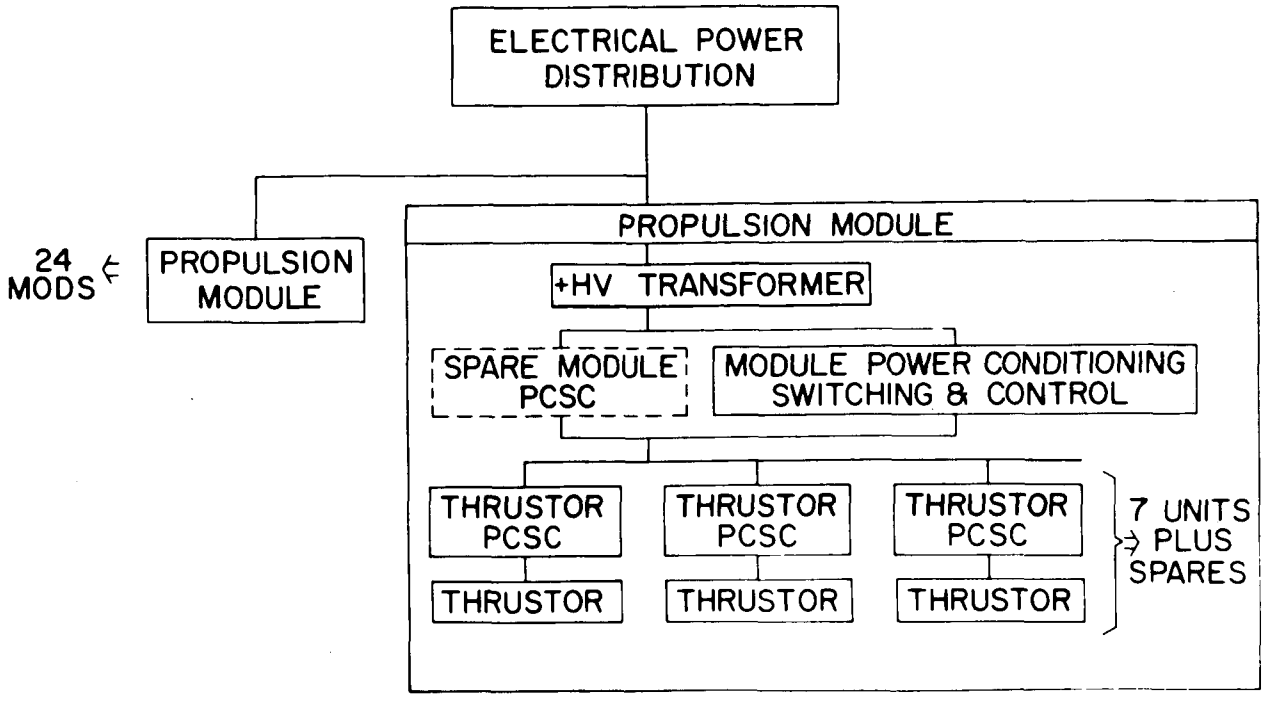

Figure 18. Electric Propulsion Reliability Schematic

The nominal component reliability data assumed for this first cut study are listed in Table 1. The reactor core data is consistent with SNAP-8 design objectives and experience. The reliabilities assumed for the reactor controls and power conversion controls assume human access for minor maintenance and repair, which can readily be provided. The use of electromagnetic pumps is assumed throughout the system; the failure rates are suspected of being conservative since, although many such pumps have been operated, failures have rarely occurred. The radiator armor weights and failure probabilities are based upon the Whipple 1963A meteoroid environment and the 1964 NASA Lewis Research Center puncture criterion. The remaining data are rough estimates believed to be consistent with ordinary space hardware reliability levels and test program budgets.

The analysis proceeds in three major steps. The first is the selection of several nominal system configurations which vary in the number of redundant components provided, and hence in both specific weight and degree of probable power decay. The second is

TABLE 1. NOMINAL UNIT RELIABILITY DATA

Item	Failures per million hours	Reliability for 10,000 hours
Reactor Core	1.0	0.99
Reactor Controls	0.3	0.997
Large EM Pumps	1.0	0.99
Small EM Pumps	0.3	0.997
Reactor Assembly		
Auxiliary Radiator	0.25	0.9975
Boiler	2.0	0.98
Turboalternator	2.0	0.98
Condenser	2.0	0.98
Power Conversion Controls	1.0	0.99
Power Conversion		
Auxiliary Radiator	0.5	0.995
Primary Radiator Segment	7.0	0.932
Ion Thrustor	5.5	0.95
Thrustor PCSC	8.3	0.92
Transformer	0.5	0.995
Module PCSC	2.8	0.973

the selection of a reliability level for the nominal mission, as opposed to the crew survival probability, and the third is the selection of the nominal configuration which results in minimum vehicle gross weight and power for the assumed mission and the selected reliability level. This process is detailed in Volume II. The result of the first step was the selection of the set of 5 configurations listed in Table 2.

Each of these configurations has associated with it a probable time history of delivered power as illustrated in Figure 19. Each curve in this figure is defined as follows: at each time point there is at least a probability P that the actual power will not be less

TABLE 2. SELECTED CONFIGURATIONS

System configuration number	1	2	3	4	5
Power conversion configuration	1	1	2	4	5
Spare control sets per PCU	0	0	1	1	1
Spare aux. radiator pumps per PCU	0	0	0	1	1
Spare condensate pumps per PCU	0	0	0	1	1
Spare primary radiator pumps	0	0	0	0	1
Spare primary radiator segments per powerplant	0	2	4	6	6
Spare module PCSC per module	1	1	1	1	1
Spare thrustors per module	0	1	1	2	2
System specific wt in kg/kwe	16.37	16.70	17.04	17.54	18.11
Energy Fraction at P = 0.9	.870	.915	.925	.949	.960

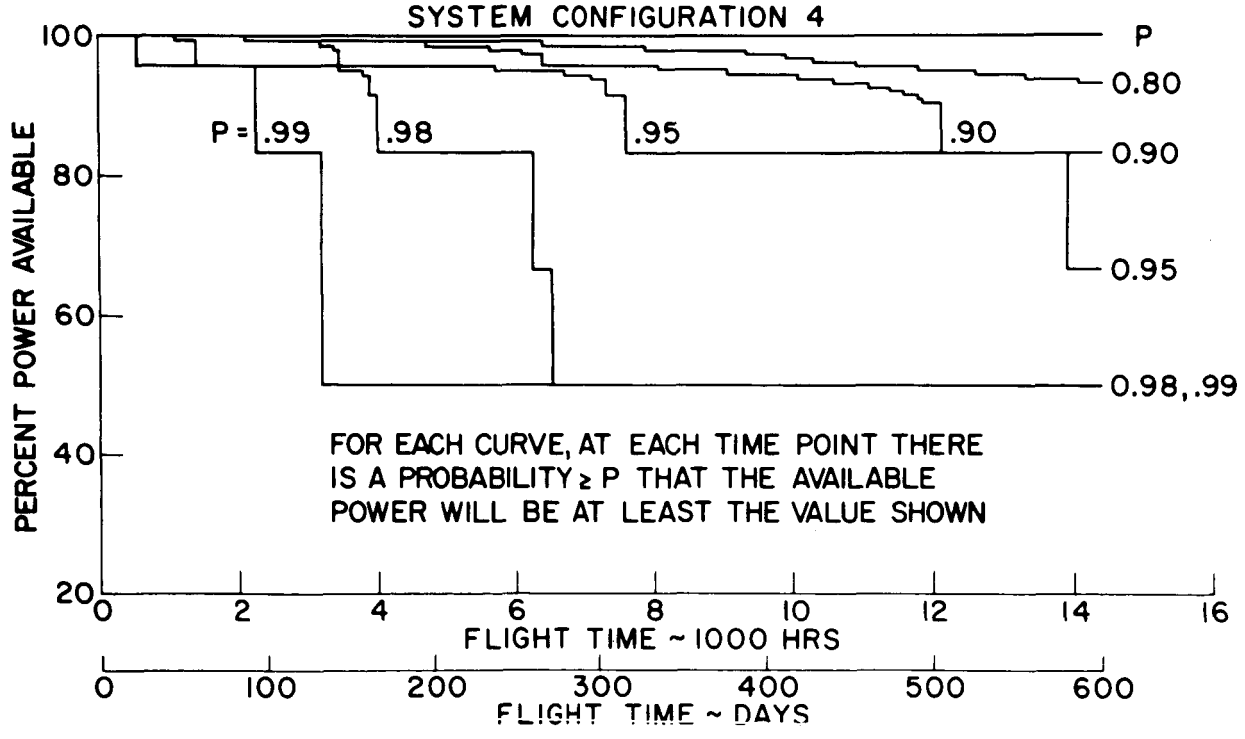

Figure 19. Typical Power Profile

than the power shown.

Under the original assumptions the system can only operate at descrete power levels; hence, the step function curves. For example, the 99.4 percent power level represents loss of one thrustor beyond the spares provided in one of the propulsion modules. Similarly, the 97.2 percent power level corresponds to the loss of one primary radiator segment beyond the spares provided in one powerplant. The 83.3 percent power level could be caused by the loss of 28 thrustors (either through the loss of up to four complete propulsion modules or the loss of the individual thrustors in various combinations), by the loss of eight primary radiator segments beyond the spares provided, or by the loss of two of the four power conversion units in one powerplant. The $P = 0.9$, $P = 0.95$ and $P = 0.98$ curves are observed to drop sharply to this level and remain there for some time; this is due primarily to the failure probability of the power conversion units. The conclusion, then, is that the level of reliability assumed for these units is near the lower end of the acceptable region. The $P = 0.98$ and $P = 0.99$ curves show a similar sharp drop to 50 percent power. This is due almost entirely to the assumed failure probability of the reactor core itself and to the assumption that the core either is working and can deliver any power up to full power, or has failed and can deliver no power. It follows that if this is a good reliability model of the core, one must provide at least the two reactors assumed here. However, experience indicates that the model of this particular item may be quite poor, and it then follows that a careful investigation of the reliability characteristics (especially the probable failure modes) of the core is very much in order.

Continuing with the present case, it is observed that values of P as high as 0.9 can be reached with relatively small power decline penalties, but that higher values of P imply markedly increased power drop. It is therefore concluded that for this investigation a P of 0.9 is a reasonable choice. This means that a vehicle designed to fly an optimum trajectory based upon the $P = 0.9$ power profile would have on the order of a 90 percent probability of being able to fly essentially its nominal trajectory, and abort flight plans must be provided to cover the possible power losses beyond the ones assumed. Low

thrust abort trajectories are under continued investigation; however, it appears at this point in time that the required abort capabilities can be provided. The curves show that the dual powerplant configuration used provides a very high probability that at least one powerplant will continue to operate throughout the mission. It is shown in Section 9 that in many cases it is possible to get back to the Earth on markedly reduced power provided that the trip time can be extended. Figure 20 shows the P = 0.9 power profiles associated with the system configurations listed in Table 2. The degree of power decay associated with each curve can be expressed as an energy fraction, the ratio of energy actually delivered to that which would be delivered if full power were obtained throughout the mission; this data is included in Table 2. The next step is the translation of this data into vehicle weight and power using the methods of Section 2. A 600 day return to Earth orbit mission was assumed. The results of the optimization are shown in Figure 21. Configuration 4, which has an energy fraction of 95 percent and a terminal power 83 percent of its initial power, is observed to be the best choice.

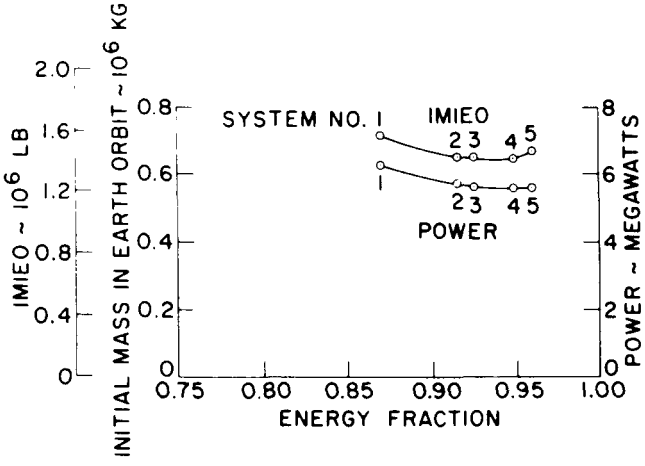

Figure 20. Nominal Power - Time Curves P = 0.9

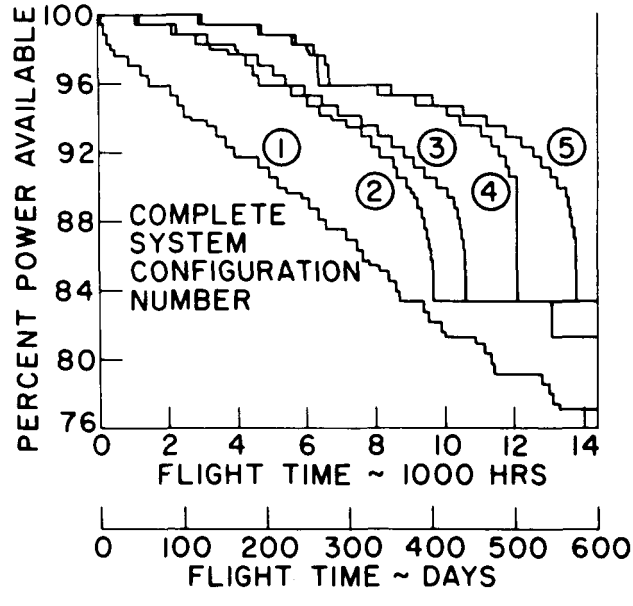

Figure 21. Reliability Optimization

A comparison case was also run in which all of the reliability features (except the use of dual powerplants) were deleted. The power conversion units were scaled down to remove the 33 percent reserve capacity assumed above, the radiator armor was removed, and all redundant components were removed. This resulted in a 17 percent reduction in the complete system specific weight from that of System No. 4. Coupling this with 100 percent power for the complete mission (an essentially zero reliability case) yielded a required initial mass in Earth orbit of 448,000 kg (989,000 lb) and a power level of 4.63 megawatts. The input assumptions regarding reliability are observed to produce a vehicle weight penalty of about 40 percent.

The quantitative data shown above obviously reflects the initial assumptions, especially the component reliabilities of Table 1, and hence must be regarded as only the grossest estimate. As time progresses and knowledge increases, one would expect both the reliability models and the input data to change, and hence the numerical outputs would also shift. However, some reasonably firm qualitative conclusions can be drawn from these present results. The first is the (not unexpected) result that the best strategy for achieving the required overall reliability must involve all of the standard approaches, including the design of the nominal trajectory for a declining power profile and the inclusion of a weight penalty for reliability assurance in both the powerplant and the electric propulsion system. The declining power profile can be regarded as a particular form of derating in which the powerplant and propulsion combination begins the mission at full rated power, but with a high probability that component failures enroute will gradually degrade the power and available thrust. The nominal trajectory and, in fact, the entire design reference mission, are based upon the assumption that these failures will occur; by this means one achieves a high probability of being able to complete the design mission. The weight penalty for reliability assurance thus comes in two ways; first, propellant weight and system operating time increases due to the declining power profile and, second, powerplant and propulsion specific weight increases due to spare parts and derated (in the usual sense) components. Note that in implementing the last item one does not simply scale up the entire plant, but instead one selectively builds up

the weak points, particularly the many components which have a small specific weight and a high failure rate.

The second conclusion is that the vehicle gross weight penalties associated with achieving high reliability with Rankine cycle nuclear electric vehicles may be significant, perhaps on the order of 40 percent, and therefore the reliability area is one which deserves considerable attention in future studies. However, the penalties are not so severe as to remove the nuclear electric vehicles from contention, as they enjoy a marked weight advantage over high thrust vehicles even with the reliability bogey (see Section 9).

The third conclusion is that the reactor core itself is a critical reliability item in the sense that its failure modes must be carefully defined and realistically represented in any future studies along these lines. This conclusion has been underscored by other studies which have shown that a single reactor-single powerplant vehicle would have a 30 percent lower powerplant specific weight (due to reduced shielding) and, correspondingly, as much as a 50 percent reduction in vehicle gross weight compared to the dual powerplant vehicle. Ranking immediately behind the need for a better reliability model of the reactor core is the need for operating experience with complete power conversion units.

The final conclusion is that the methods employed in this example analysis (see Volume II) constitute a useful initial approach to the reliability problem of manned nuclear electric vehicles. The primary feature of this approach is the integration of the reliability calculation and optimization into the overall vehicle and trajectory optimization; such an integration has been found to be essential to any attack on the problem, even at this early stage.

SECTION 7

NUCLEAR VEHICLE DESIGN

Two overall vehicle design layouts have been prepared in the study to date. The first vehicle is a 4.9 Mwe single powerplant vehicle designed for a 1981 600-day hyperbolic return mission. The vehicle sizing and optimization was performed with a preliminary vehicle/trajectory model which subsequent study has shown to be deficient. The latest data, obtained with a new vehicle/trajectory model, indicates that this vehicle is off optimum in its proportions and somewhat undersized for the design mission. However, it does serve to illustrate several aspects of vehicle design and integration and it has yielded valid subsystem weight data. It is presented here in that light.

Figure 22 shows the launch and orbital assembly sequence for this vehicle while Figure 23 shows the vehicle in its interplanetary flight configuration. As shown, the vehicle is launched in four 10 m (33 ft) diameter Saturn V payload packages. The first package contains three quarters of the electric propulsion system and the Mars excursion module. The second package contains the nuclear powerplant and the mission module. The third contains the remainder of the electric propulsion system, the Earth entry module, and a tank of liquid hydrogen for the Earth departure stage. These three are assembled as shown in low Earth orbit. A full power test of the powerplant and electric propulsion system is then carried out. After a successful checkout, the power is cut back and the final launch package (the main hydrogen tank and nuclear rocket) is launched and mated, whereupon the vehicle is ready for departure. In interplanetary flight the mission module is deployed on a folding, telescoping boom. Artificial gravity is provided by rotating the vehicle propeller-fashion around the thrust vector as shown in Figure 23.

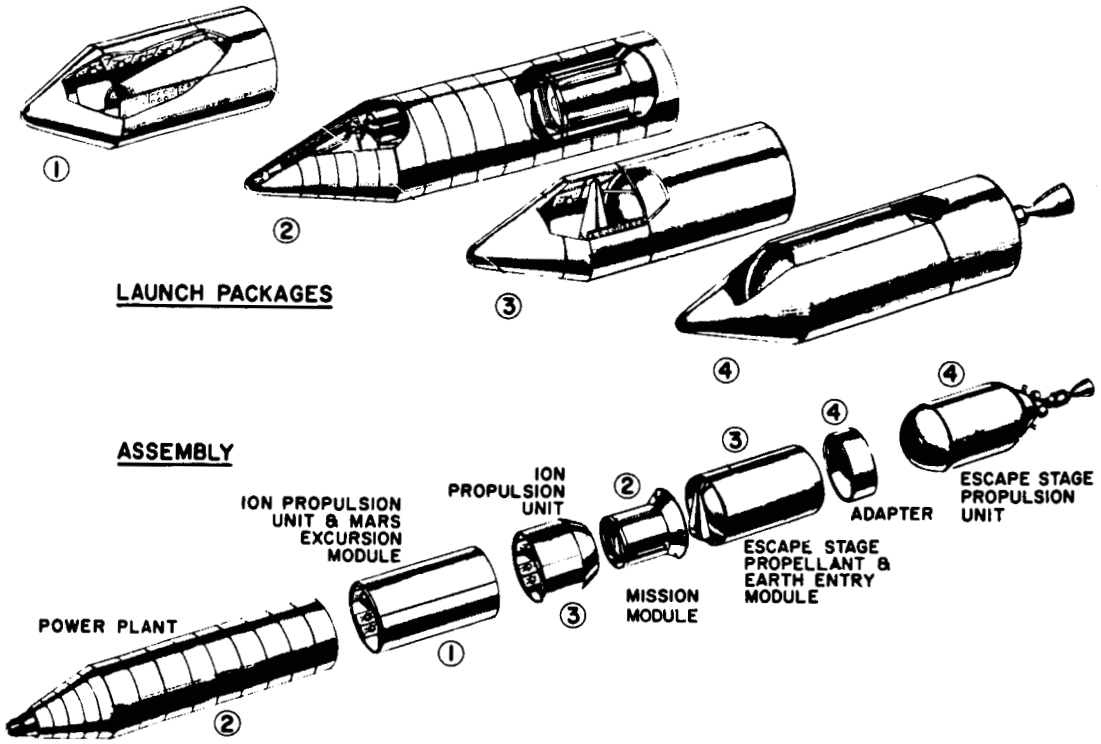

Figure 22. 4.9 Mw Launch and Orbital Assembly

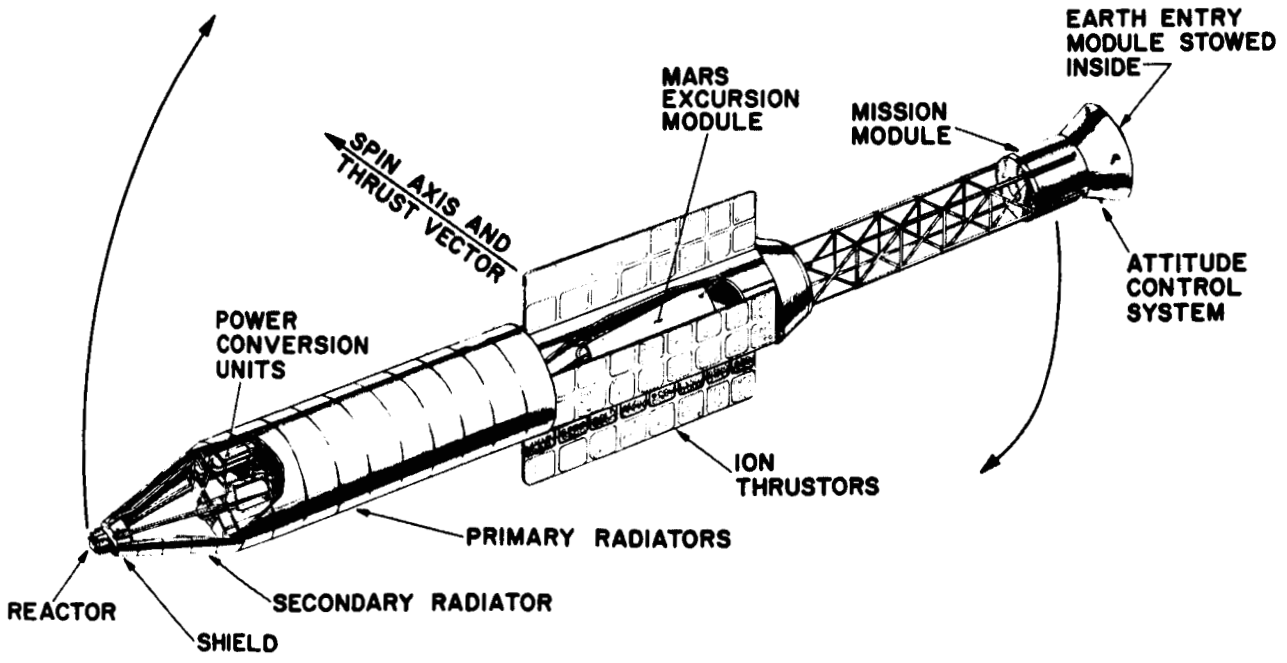

Figure 23. 4.9 Mw Vehicle Interplanetary Flight

The initial mass in Earth orbit is 449,000 kg (990,000 lb), the initial nuclear-electric spacecraft weight is 249,000 kg (550,000 lb), and the weight at Earth return (just prior to the Earth entry module separation) is 132,000 kg (290,000 lb). The powerplant specific weight is 13.6 kg/kwe (30 lb/kwe). A total of 768 state-of-the-art level one electron bombardment thrustors (576 operating, 192 spares) are used to produce 143 Newtons (32.2 lb) of thrust at a specific impulse of 4750 seconds. The total weight of the thrustors and their support structure represents a specific weight of 2.2 kg/kw (4.8 lb/kw). The power conditioning adds another 1.9 kg/kwe (4.2 lb/kwe). The tankage and tank support structure weight is 10 percent of the propellant weight. The six man Earth entry module weight is 7300 kg (16000 lb), the mission module weight is 38,000 kg (83,800 lb) and the Mars excursion module weight is 30,400 kg (67,000 lb).

The second vehicle is a two powerplant, 8 Mwe vehicle designed to return to a 100,000 km Earth orbit at the end of a 792-day mission. The overall arrangement of the vehicle is shown in Figure 24 and in the Frontispiece. The launch packaging and assembly of the electric propulsion system is shown in Figure 25. The assembly of the vehicle into the Earth departure configuration is shown in Figure 26. Each of the first three Saturn V launches carries one arm of the electric propulsion system; these arms are then connected together as shown. The next launch carries one powerplant with the mission module inside (in the manner of Figure 22). The mission module attaches to one arm of the propulsion system and the powerplant to another. The fifth launch brings the other powerplant and the Mars excursion module. The next four launches each bring a unit of the Earth departure stage and its connecting structure. After attaching the departure stage to the interplanetary vehicle, the two powerplant arms are folded as shown to relieve bending loads during the departure propulsion. Like the 4.9 Mwe vehicle described above, this vehicle provides artificial gravity during interplanetary flight by deploying the mission module and rotating the vehicle around the thrust vector.

The initial mass in Earth orbit is 800,000 kg (1,763,000 lb), the initial nuclear-electric spacecraft weight is 420,000 kg (925,800 lb), and the Earth return weight is 199,000 kg

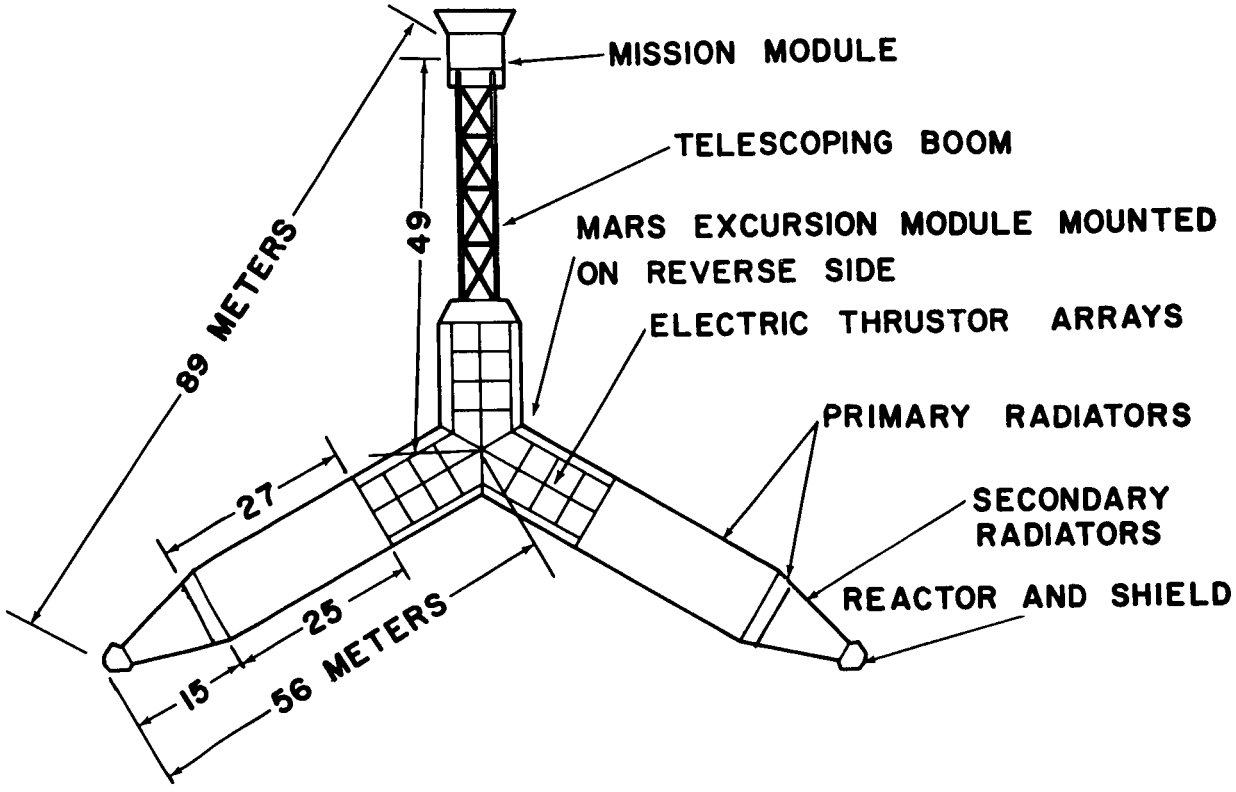

Figure 24. 8 Mw Vehicle Concept Interplanetary Configuration

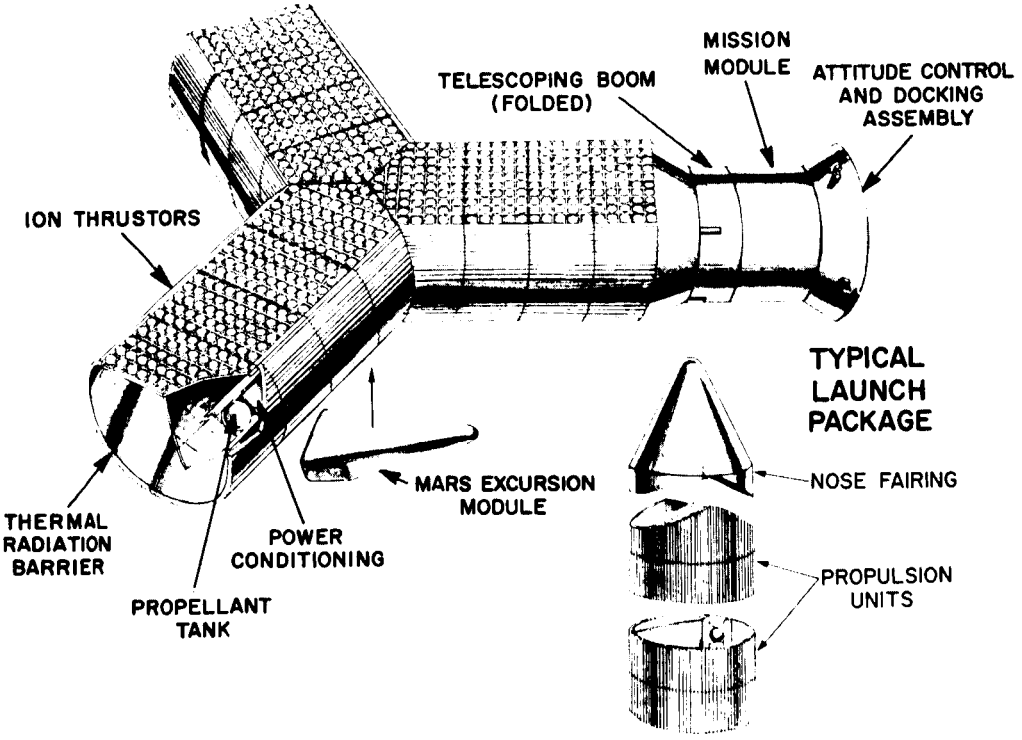

Figure 25. Propulsion System Design

I

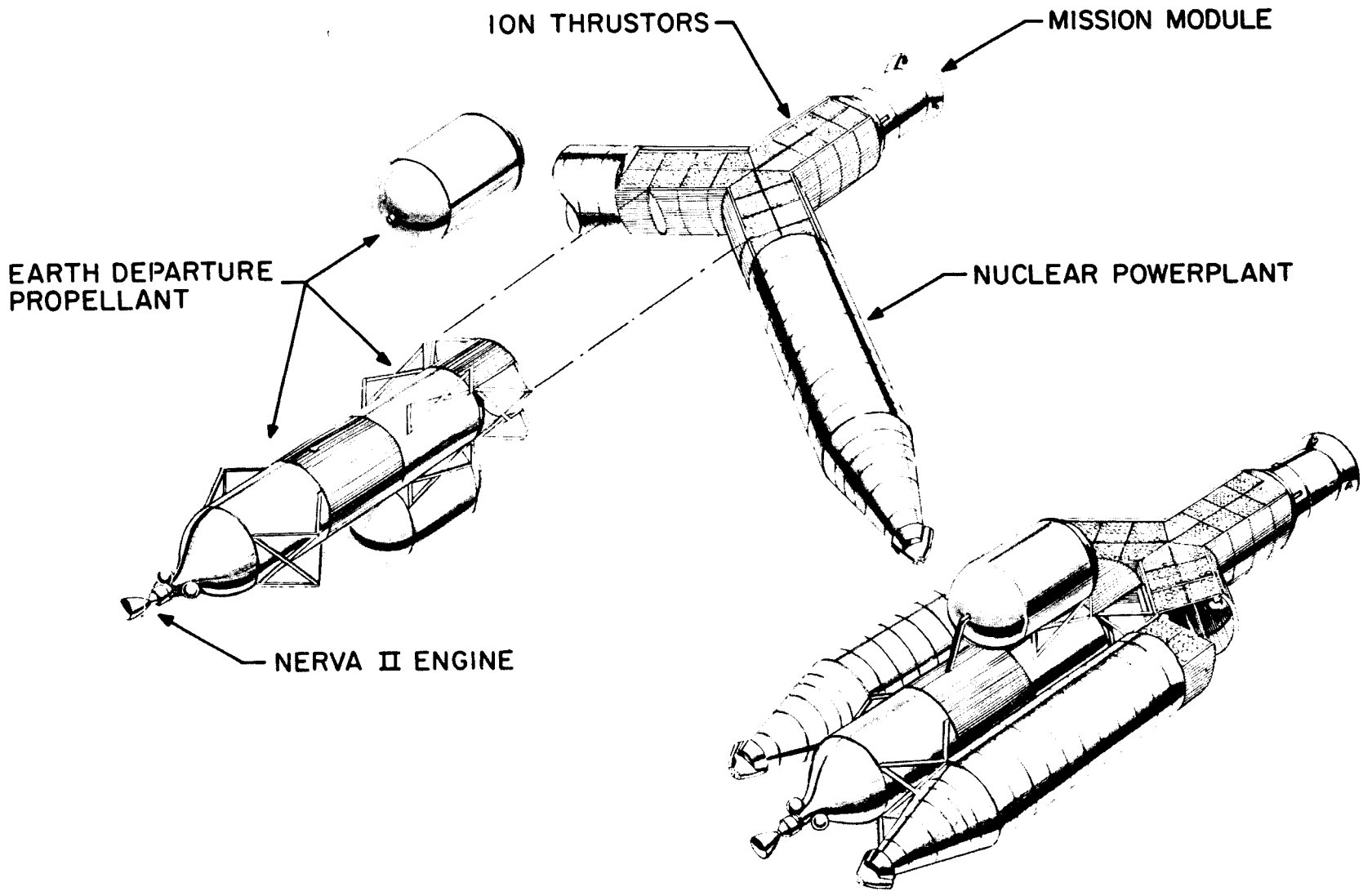

Figure 26. 8 Mw Vehicle Orbital Assembly

(440,000 lb). The powerplant specific weight is 15 kg/kwe (33 lb/kwe). A total of 600 state-of-the-art level 2 electron bombardment thrustors (456 operating, 144 spares) provide 194 N (43 lb) of thrust at a specific impulse of 5800 seconds. The thrustors and their support structure represent a specific weight of 1.13 kg/kw (2.48 lb/kw). Again, the power conditioning was assumed to weigh 1.9 kg/kw (4.2 lb/kw). The tankage and tank support structure weight is 3 percent of the propellant weight. The mission module weight is 44,900 kg (99,000 lb) at Earth departure while the Mars excursion module weight is 30,400 kg (67,000 lb).

The weights and performance above are based upon the use of a 550 km orbit at Mars and upon an early, heavy mission module. With the 8 man mission module weights of Section 3 and the use of a 17,000 km synchronous orbit at Mars, this vehicle could perform the round trip in 500 days.

Even beyond this, however, the large specific weight penalties (and resultant vehicle performance penalties) of the dual powerplant concept have led to the conclusion that the next phase of study should be focused upon a single powerplant vehicle concept similar to the one shown in Figure 27 and 28. A single in-orbit mating of two radiator sections is postulated to circumvent the launch vehicle payload length limits and permit both a minimum weight (not area limited) radiator and a small cone angle (minimum shield weight). Such a concept should lead to performance similar to that shown for the 10 kg/kw powerplant in Figure 41, page 9-13.

The concept would ideally use a single reactor. A careful study of the reliability implications of this would, of course, be a major part of its investigation. It is suspected that, since the reactor consists of many separate fuel elements, a highly reliable pressure vessel, and controls which can be made redundant or replaceable, adequately high reliability may well be achieved.

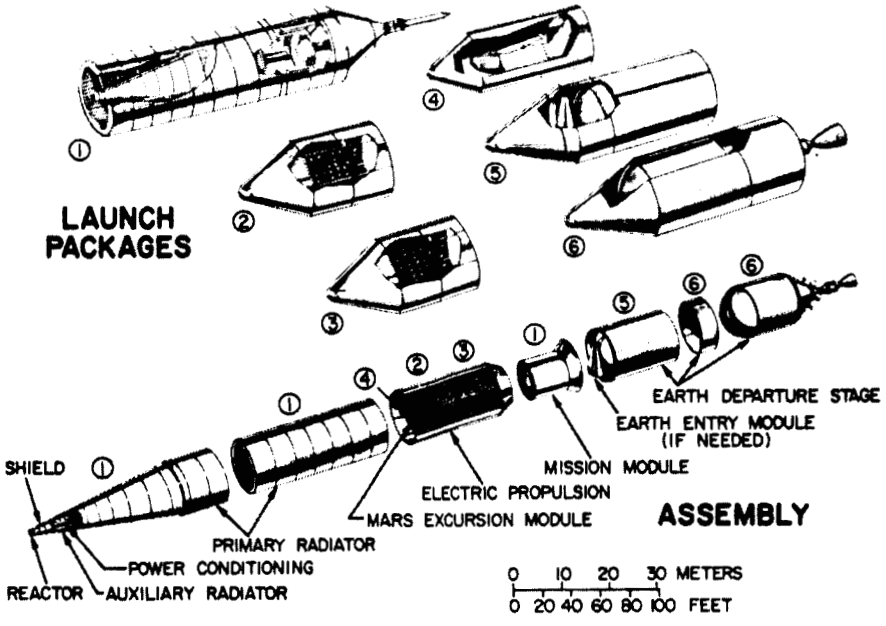

Figure 27. Single Powerplant Vehicle - Orbital Assembly

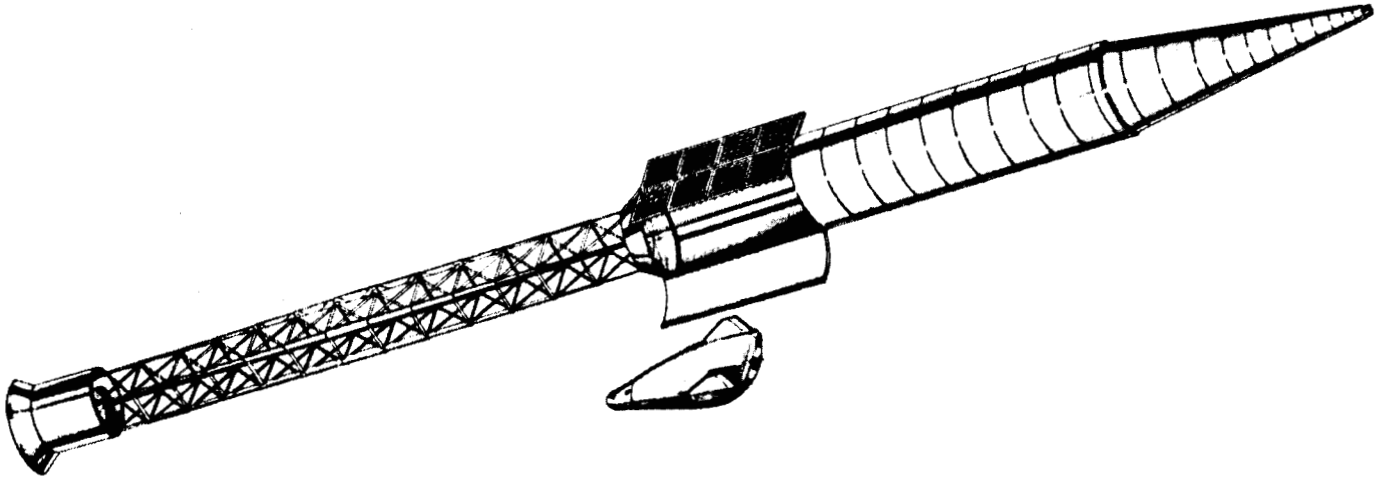

Figure 28. Single Powerplant Vehicle - Mars Orbit

SECTION 8

SOLAR-ELECTRIC VEHICLE DESIGN

The feasibility study of solar-electric manned Mars vehicles has proceeded in 3 concurrent lines of effort. The first (and largest) is the development of the required performance analysis tools as described in Section 2. The second is the definition of the array properties; cell weight and efficiency, substrate weight, and electrical network weight. The third deals with the deployment structure and overall vehicle design.

The basic solar cell assumed is a 2 x 2 cm silicon cell 0.2 mm (8 mils) thick with an efficiency of 10% (AMO). A 0.1 mm (4 mil) cover glass is assumed, and the cell is assumed to be bonded to a 0.1 mm (4 mil) film substrate. The total weight of a 2 x 2 cell assembled with its cover glass, substrate, and intercell electrical connections is estimated to be 0.4 grams. The buildup of such cells into a major array segment is illustrated in Figure 29; note the added bus bar weight at each step.

The basic requirements of a solar-electric manned Mars vehicle are the following:

1. The solar array must be continuously oriented toward the sun.
2. The thrust vector direction with respect to the array must be variable over a wide range, including the ability to thrust on either side of the array.
3. Artificial gravity through rotation of the mission module is highly desireable.
4. Crew access to the electric propulsion system for in-flight maintenance and repair is required.
5. A high thrust (0.1 to 0.2 g) departure from the Earth assembly orbit will be used.
6. A full power operating checkout is required prior to Earth departure.

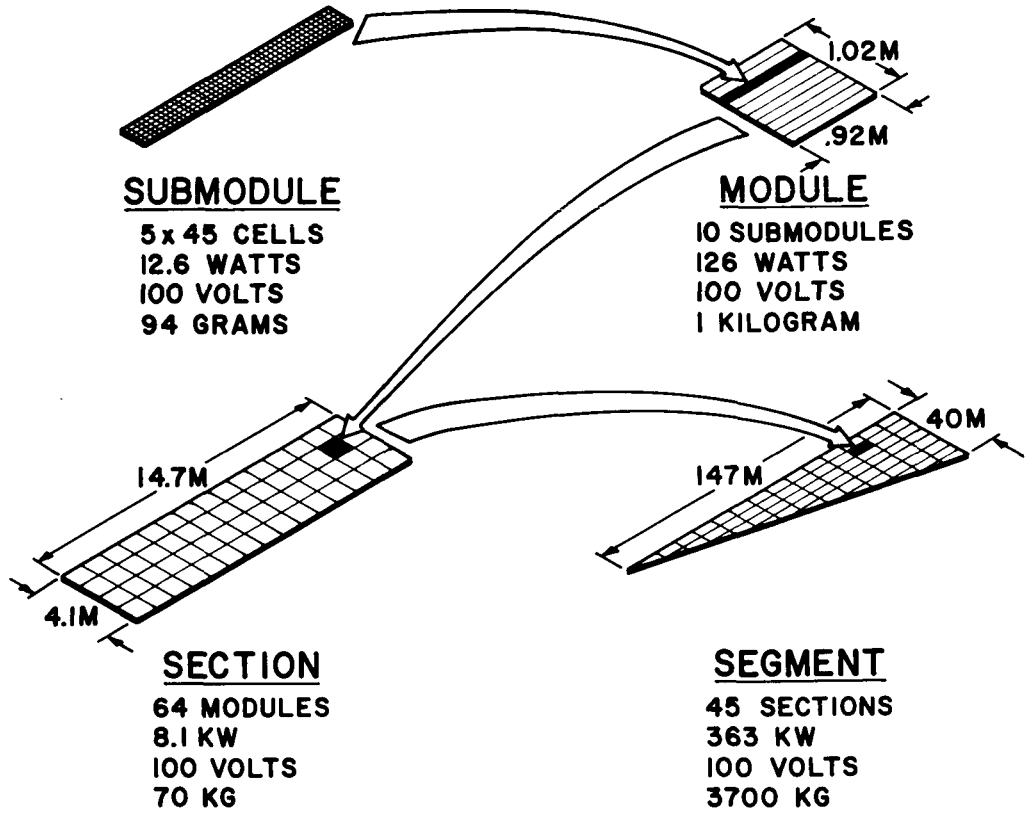

Figure 29. Array Segment Buildup

Performance studies have shown that a substantial performance gain may be achieved through the use of high thrust at Mars and this possibility merits full exploration in future work. To date, however, the use of all low thrust Mars capture and departure has been assumed to avoid the need for folding the array at Mars or strengthening it to withstand the acceleration loads.

A little arithmetic quickly shows that a multi-megawatt solar array is truly enormous; perhaps 200 to 400 meters across. Figure 30 shows a promising concept for deploying such an array while satisfying the above requirements. The vehicle in its interplanetary configuration (same as the checkout configuration in Figure 30) is basically non-rotating. Artificial gravity is provided for the crew by rotating the pair of mission module units around the central body of the vehicle. The electric propulsion system can be re-oriented by rotating it around the central body. This, coupled with the ability to re-orient the entire vehicle by rotation around the vehicle-sun line, provides complete freedom of thrust vector orientation.

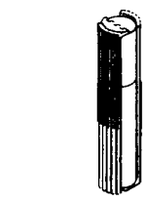

1-LAUNCH CONFIGURATION

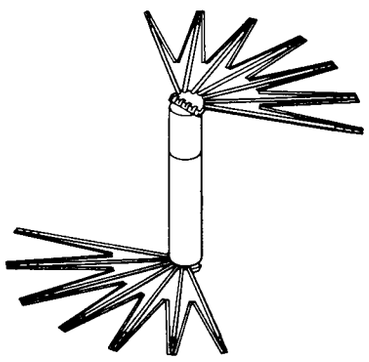

2-FIRST UNFOLDING

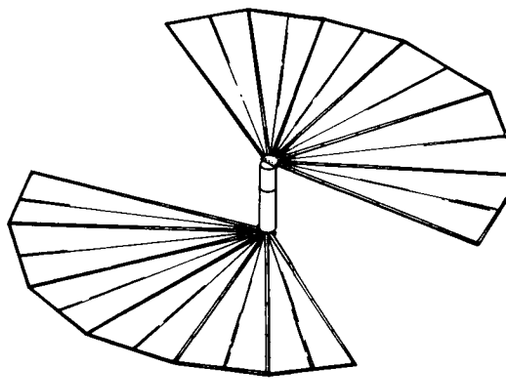

3-BOOM EXTENSION

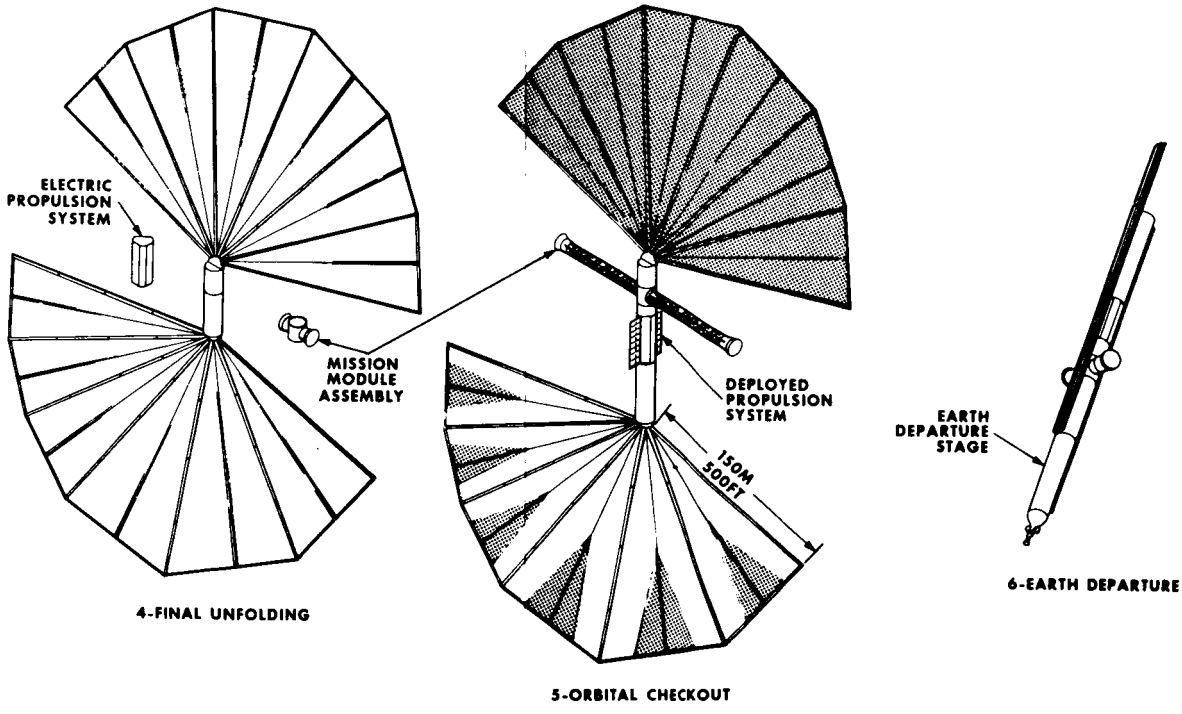

Figure 30. Deployment Concept

The deployment proceeds through a sequence of unfolding and extension of telescoping spokes until the framework is set, and then culminates with the unrolling, window shade fashion, of the solar cell array segments. It is observed that the idea of mounting the array segments on a film substrate and rolling them up for launch permits the packaging of up to an 8 or 10 megawatt array on a standard Saturn V. The array rollers and spokes are hollow cylinders of aluminum honeycomb deployed by small electric motors. Their strength has been found to be adequate to withstand ground handling loads, launch loads (in the telescoped configuration supported by the central structure) and the steady state in-flight loads. The response of the vehicle to dynamic loads (e.g., an imbalanced pair of mission module units) is not known yet and could be a major problem. The power source weights associated with this vehicle concept are listed in Table 3.

TABLE 3. TYPICAL SOLAR POWER SOURCE WEIGHTS

CELLS	17,400 KG	38,400 LB
GLASS	8,900	19,600
BOND	1,900	4,200
FILM	5,800	12,800
ELECTRICAL CONNECTORS	3,400	7,500
ELECTRICAL NETWORK	17,300	38,100
TOTAL ARRAY	54,700	120,600
SPOKE STRUCTURE	10,100	22,300
DEPLOYMENT MOTOR ASSYS	800	1,800
ROLLERS	1,700	3,700
CENTRAL STRUCTURE	1,800	4,000
TOTAL POWER SOURCE	69,100 KG	152,400 LB

SPECIFIC WT @ 1 AU = 13
@ 1.5 AU = 23.6
KG/KW = 28.6 LB/KW
KG/KW = 52 LB/KW

NON-ROTATING ARRAY
AREA = 42,900 m^2 = 462,000 FT^2
POWER = 5.3 Mw

An alternative vehicle concept in which the mission module was attached rigidly to a circular array and the whole array was rotated for artificial gravity was analyzed as described in Volume II. The centrifugal force field significantly stiffens the array, but the concept suffers from a major limit on thrust vector direction and from several potentially severe dynamics problems. As a result the concept has been abandoned.

Volume II discusses some tentative explorations which have been made as to the design implication of high thrust operations at Mars. These have been conclusive only in showing that there are major vehicle-performance interactions which require more than quick estimates for their resolution.

SECTION 9

VEHICLE PERFORMANCE

The revised Manned Mars Mission Model of Section 2 has been used in conjunction with the LEADER optimization technique to investigate the effects of the major system design parameters and a number of operational options on the overall system performance characteristics. Additional performance data have been developed to permit a direct comparison between hybrid nuclear rocket-nuclear electric propulsion and the more conventional high thrust chemical and nuclear rocket propulsion systems. All of the data reflects the general mission profile as shown in Figure 1. However, it is noted that the individual parametric studies are not, in general, based upon a common list of basic inputs. This is particularly true with respect to the weights of the Mars excursion module (MEM) and the mission module, the staging orbit altitude at Mars, the reference trip time, and the Earth return mode. This is a direct consequence of the continual evolution of the mission concept as a result of the parallel system studies and parametric studies. Additional, more detailed parametric optimization studies using a common base point are planned for the subsequent study phase of this program.

The following sections summarize the results of the parametric optimization studies completed to date.

9.1 NUCLEAR ELECTRIC PARAMETER STUDIES

Figure 31 illustrates the variations in initial mass in earth orbit (IMIEO) and power rating with round trip time for an optimized power level and for a fixed power level of 8 Mw. These data are based upon a 1981 Earth departure, a powerplant specific

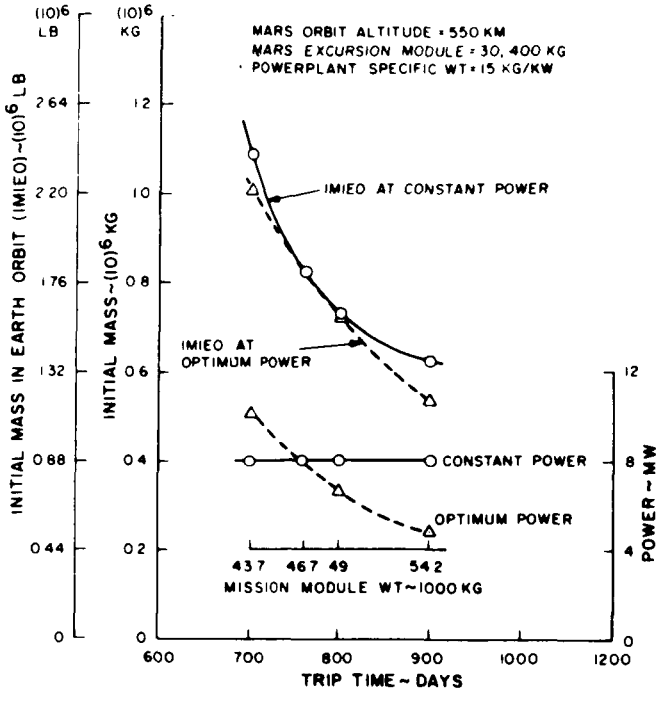

Figure 31. Trip Time Effect at Constant Power

weight of 15 kg/kw (33 lb/kw), a Mars orbit altitude of 550 km, a MEM weight of 30,400 kg, (67,000 lb) and a terminal Earth orbit altitude of 100,000 km. The 8 Mw power level is optimum for a trip time of 762 days. Note that the variation in IMIEO requirements between the optimum power line and the constant power line is less than 12% over the trip time range of 700 to 900 days. Optimum power requirements over this range vary from 4.8 to 10.2 Mw. This insensitivity of overall system weight to design power level implies that in many cases development planning, launch packaging and orbital operations factors can be allowed to limit the power level without incurring a major penalty.

Figure 32 summarizes the effects of variations in Mars orbit altitude on the optimum IMIEO and power requirements. These data are based upon a round trip time of 762 days, a mission module weight of 46,800 kg (103,000 lb), a powerplant specific weight of 15 kg/kw (33 lb/kw), and on a terminal Earth orbit altitude of 100,000 km. Data are indicated for MEM descent and ascent propulsion based upon storeable propellants with specific impulse capabilities of either 310 or 360 seconds. The corresponding MEM weights are tabulated for each case, as obtained from the studies recorded in Section 3. Additional data on Mars orbit altitude effects are shown in the Figures 38 and 39.

These results indicate that both the IMIEO and the power requirements are reduced as the staging Mars orbit altitude is increased. This trend with increasing altitude is the result of a trade-off between increasing MEM propulsion requirements at the low

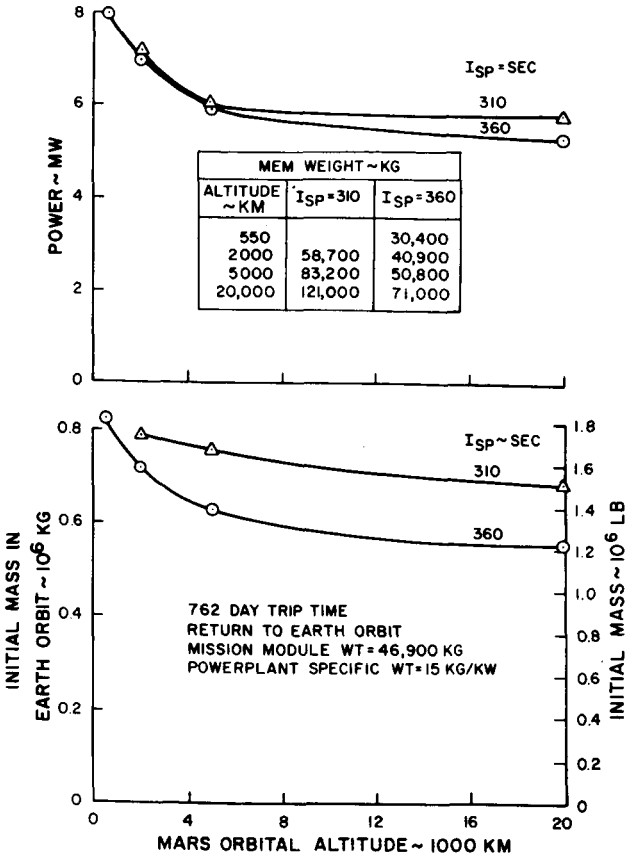

Figure 32. Mars Orbital Altitude Variation: Nuclear Powerplant

specific impulse levels of storeable propulsion systems and decreasing heliocentric propulsion requirements of the nuclear-electric system as the savings in the low thrust spiral time at Mars is added to the available heliocentric trip time. On the basis of these results the base point for the subsequent parametric studies was revised to use a MEM weight based upon the use of the 360 seconds specific impulse system in conjunction with a Mars orbit altitude of 20,000 km.

The high orbit has both advantages and disadvantages from an operational viewpoint. The disadvantages are 1) increased MEM guidance accuracy required, 2) decreased ability to observe and map the Mars surface from the main spacecraft. The advantages are 1) easier communication between the spaceship and Earth, 2) easier communication between the surface party and the spaceship, due primarily to the spaceship's being in sight a greater fraction of the total time and for longer increments of time, 3) a high ΔV MEM which might be adaptable to the role of heliocentric abort during the first month or so of the mission. The special case of a synchronous orbit (17,000 km altitude, 24.62 hour period) in constant view of the landing site is of particular interest since it would permit continuous communication between the surface party and the spaceship and essentially, if not completely, continuous communication between the spaceship and Earth. This orbit would, however, limit the mapping of the opposite side of Mars to the Mars arrival and Mars departure phases of the mission, or to an auxiliary Mars satellite launched from the main vehicle for this purpose.

The tradeoff among these operational factors is not clear at this time; however, it is tentatively recommended that a synchronous Mars orbit be assumed as the baseline for the next round of studies involving low thrust capture at Mars.

Figure 33 summarizes the results of an investigation of the effects of powerplant specific weight variations over the trip time range of 500 to 800 days. These data are based upon the Mars orbit altitude of 20,000 km and a corresponding MEM weight of 71,000 kg (156,000 lb). Mission module weights were also changed, as indicated, on the basis of the work reported in Section 3. These data indicate that in the 10 to 15 kg/kw range of interest (Section 5), very attractive vehicle gross weights are achievable with trip times of 500 to 700 days.

These data are all for a return-to-Earth-orbit mission mode. Figure 41 below contains further data on specific weight effects with heavier payloads and a hyperbolic Earth return mode. The same general effects are observed.

The consequences of discrete unplanned power losses at selected points along the mission have been investigated with respect to the base line 600 day, 15 kg/kw design. Such power losses would be representative of a loss of either powerplant or propulsion system capability as a result of subsystem failures. The following approach was used in this investigation:

a. The vehicle-mission design was fixed corresponding to the optimum design for the base line 600 day mission at 15 kg/kw powerplant specific weight.

b. A discrete fractional power loss was introduced at one or more of the following mission events; parabolic approach to Mars (capture), in Mars orbit, at parabolic departure from Mars.

c. The nominal mission specification was retained up to the time of power loss; the subsequent specifications were revised to determine the earliest Earth arrival date achievable by the nominal vehicle under the reduced power. However, in all cases the 40 day surface exploration was still carried out in full.

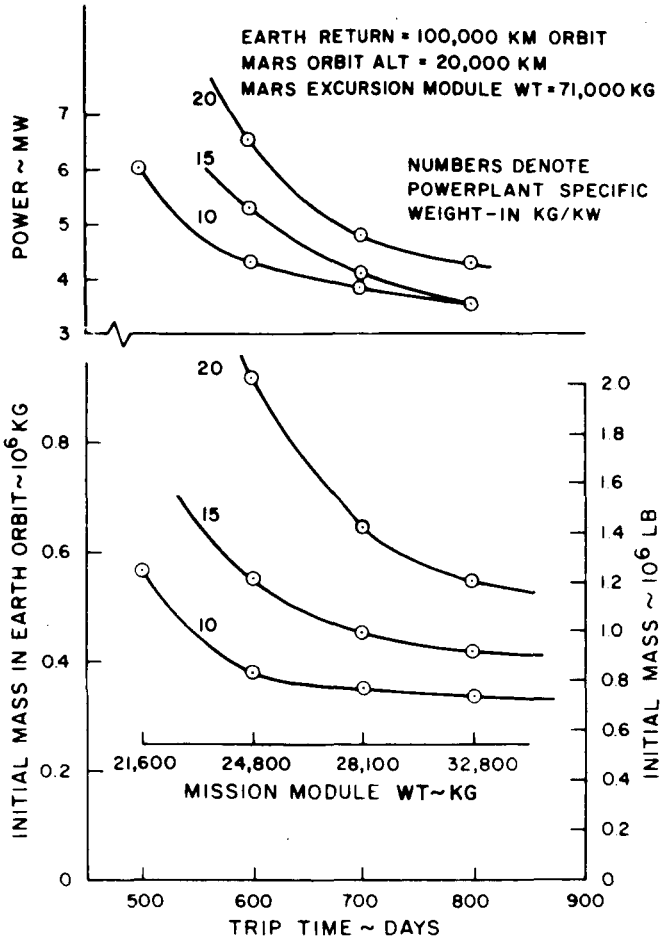

Figure 33. Effect of Specific Weight

The results of these investigations are summarized in Figures 34 and 35. Figure 34 illustrates the increased trip time requirements for various power losses at each of the above mission events. The trip time increase requirements range from 40 to 165 days with the larger values corresponding to the earlier power losses. Figure 35 illustrates the effects of multiple power failures at successive mission events. For example, a 1/8 power failure at Mars capture followed by a second 1/8 power failure at Mars departure will result in a total trip time requirement of 710 days. The first power failure, in this case, resulted in an increase in trip time of 65 days and the second failure resulted in an additional increase of 45 days.

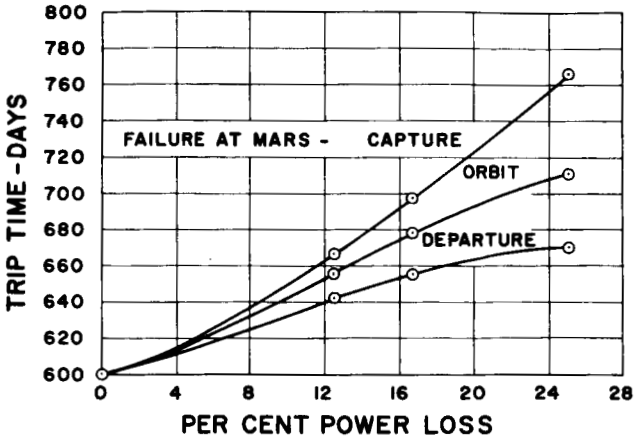

Figure 34. Effect of Unplanned Step Power Losses Nominal 600 Day Mission Powerplant

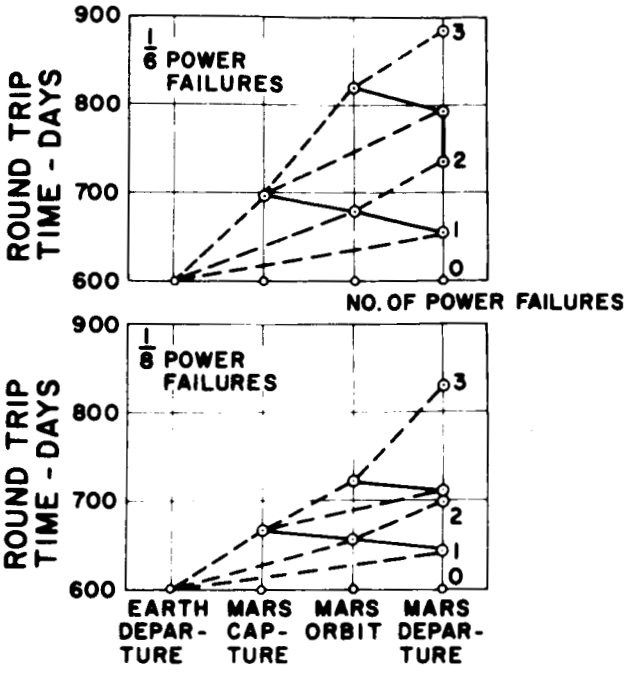

Figure 35. Effect of Multiple Power Failures Nominal 600 Day Mission

These data represent a first cut at the power loss problem in that the nominal vehicle-mission specification has been optimized for a nominal constant power profile and that the mission module weight has been based upon life support expendables compatible with the nominal 600 day trip time. A second iteration is, therefore, indicated in which the system optimization is conducted for a small planned power loss with the life support expendables sized for increased trip time associated with additional unplanned losses. It should also be noted that these data represent trip time increases associated with the full performance of the nominal MEM landing and 40 day exploration program. The increased trip times indicated for the Mars approach power losses could be reduced substantially (perhaps eliminated) by the reduction or elimination of the 40 day exploration period, or ultimately by the elimination of the capture and departure maneuvers themselves. It appears from this data that an abort procedure of extending trip time to compensate for unexpected power losses is quite useful and should definitely be part of a nuclear-electric manned Mars mission plan.

Figure 36 illustrates the effects of a continuous exponential decay (with trip time) of the powerplant capacity. These data represent cases in which the vehicle-mission specifications have been optimized for each individual power decay level as a part of the overall design strategy for maximizing both crew survival and mission success probabilities. The indicated horizontal scale represents the ratio of the terminal power to the initial power.

The resultant power curve indicates that the optimum vehicle must be altered to maintain essentially a constant terminal power level for all power decay levels. Conversely, the percent increase in IMIEO requirements is substantially greater than the corresponding power loss factor. These data are one side of the trade-off (described in Section 6) of thrustor and powerplant component redundancy versus power decay for a specified overall reliability level.

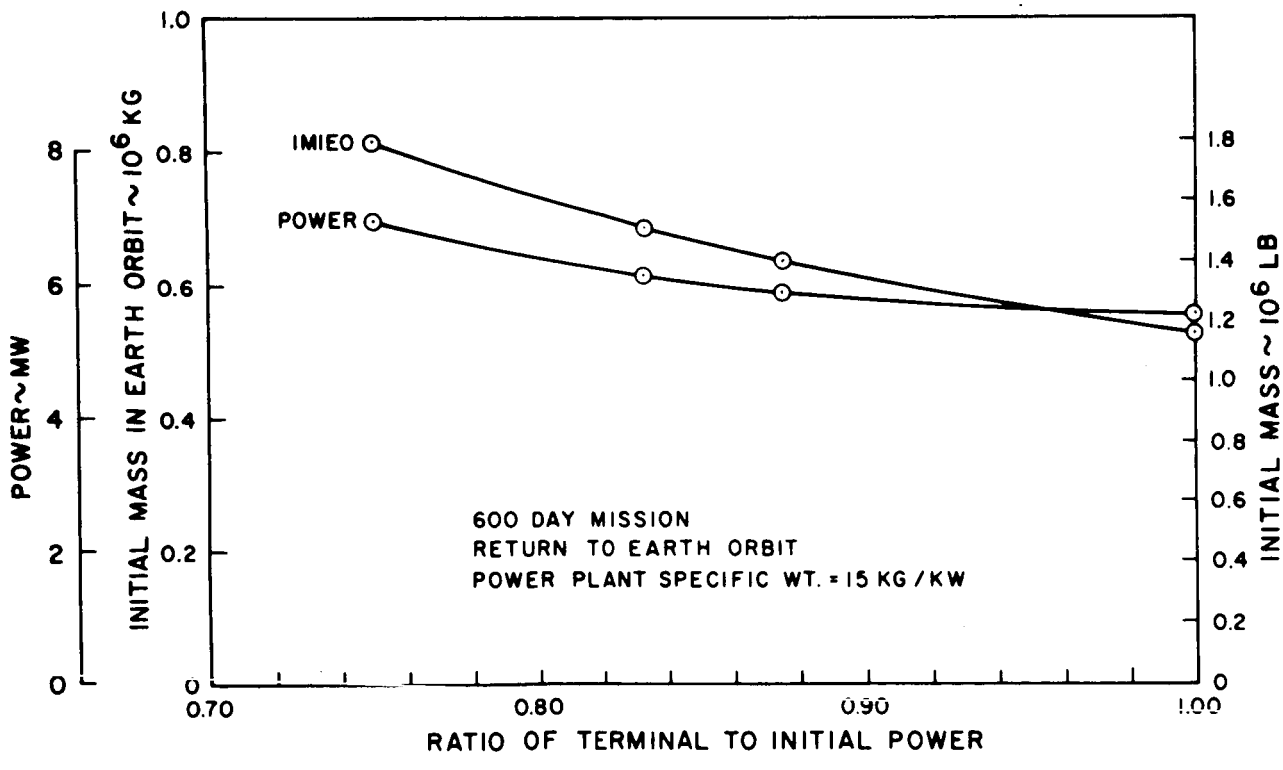

Figure 36. Planned Exponential Power Decay

9.2 SOLAR ELECTRIC PARAMETER STUDIES

Figure 37 summarizes the results of a series of solar-electric performance optimization calculations for a powerplant specific weight of 15 kg/kw. These data have been based upon a solar power decay obtained from the empirical relationship:

$$(P/Po) = 1.4\,(R/Ro)^{-2} - 0.4\,(R/Ro)^{-4}$$

Comparative nuclear-electric performance data from Figure 33 has been included. These data indicate that the solar-electric IMIEO and power requirements are essentially twice the corresponding nuclear-electric requirements at constant trip time and powerplant specific weight. Additional solar-electric performance data at a reduced powerplant specific weight of 13 kg/kw results in a 33% reduction in IMIEO and a corresponding 9% reduction in power requirements at a 600 day trip time. Further reductions in the solar-electric powerplant specific weight or a large increase in trip time would be required to reduce IMIEO requirements to the level of the nuclear-electric system.

The baseline solar-electric mission profile has assumed the following propulsion operations at Mars:

a. Low-thrust solar-electric propulsion from parabolic Mars approach to a circular orbit at the selected altitude.

b. MEM separation, descent and landing with high thrust storeable propulsion, surface exploration, and subsequent launch to rendezvous with the main spacecraft at its circular orbit altitude.

c. Low-thrust solar-electric propulsion from circular orbit to parabolic escape.

The effects of replacing a) and c) by high thrust chemical or nuclear rocket propulsion have been investigated over the orbit altitude range of 550 to 20,000 km. The following propulsion options have been investigated:

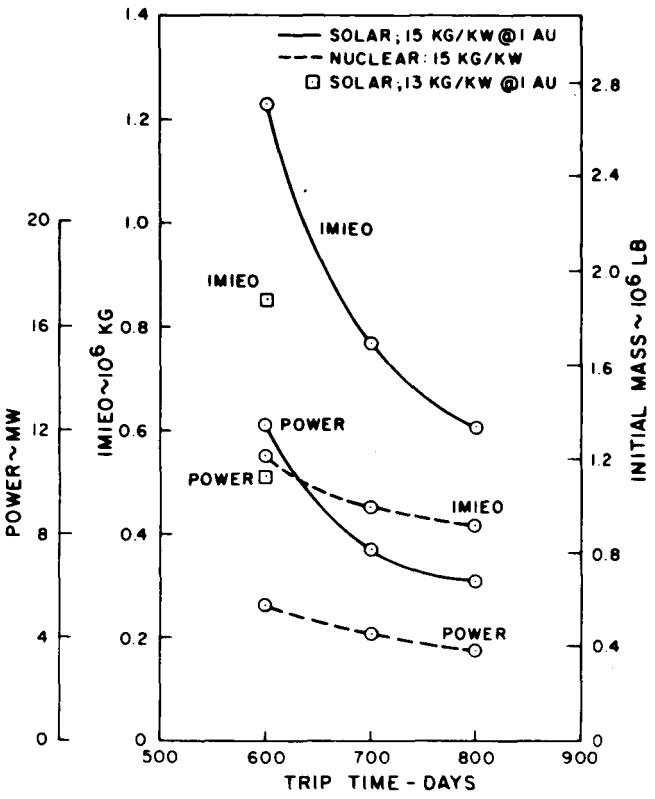

Figure 37. Solar Electric Vehicle Performance

a. Nuclear high thrust capture and solar-electric low thrust escape (NHL).

b. Nuclear high thrust capture and escape (NHH).

c. Chemical high thrust capture and solar-electric low thrust escape (CHL).

d. Chemical high thrust capture and escape (CHH).

Separate high thrust stages (engine and tankage) were used for the capture and escape phases with options b) and d). Due to limitations in the present computer program, the heliocentric propulsion approaching Mars and departing from Mars was assumed to be low thrust, terminating at parabolic approach and beginning at parabolic departure.

The high thrust propulsion system characteristics assumed for these investigations were described in Section 4.

The results of these investigations are summarized in Figures 38 and 39 for a series of 600 day solar-electric missions. Figure 38 illustrates the IMIEO variation with Mars orbit altitude for each of the four high thrust propulsion options and for the baseline all solar-electric system (SLL). Near-minimum IMIEO requirements were obtained for all propulsion options at the 20,000 km orbit altitude, the highest investigated.

At the 20,000 km orbit altitude, the replacement of the solar-electric descent mode by either nuclear or chemical high thrust resulted in a 13% reduction in IMIEO requirements. This trend is a result of the tradeoff between the reduction in heliocentric

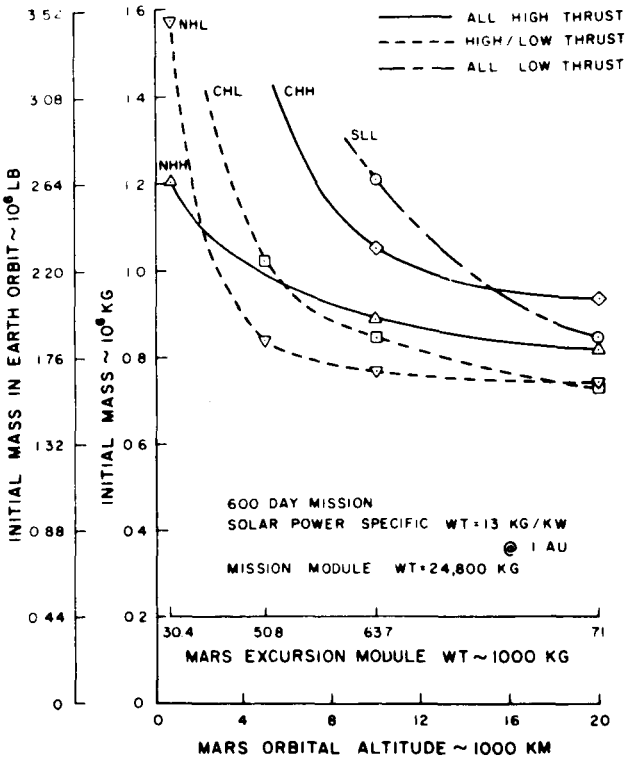

Figure 38. Effect on IMIEO of High Thrust Propulsion at Mars

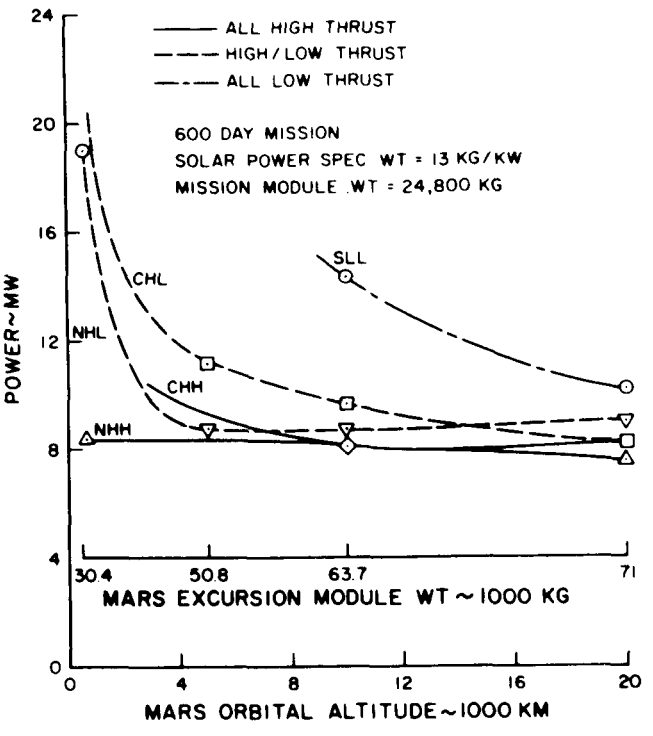

Figure 39. Effect on Power of High Thrust Braking

propulsion requirements as a result of eliminating the 30 day low thrust spiral descent period and the increased planetary propulsion requirements resulting from the performance of the descent with the substantially lower specific impulse of the chemical or nuclear rocket. Subsequent replacement of the solar-electric escape propulsion by chemical or nuclear propulsion resulted in poorer performance since it resulted in the elimination of only a 17 day spiral escape period.

The picture changes substantially, however, as the Mars orbit altitude is decreased as a result of the substantially larger propellant requirements and low thrust spiral times associated with the lower altitudes. IMIEO requirements for the CHL mode increase more rapidly than either of the nuclear modes, NHL and NHH. As a result, the NHL mode indicates the lowest IMIEO requirements down to an orbit altitude of

2000 km. Below this point, the NHH mode is best. The SLL reference mode shows the greatest IMIEO increase with decreasing orbit altitude and is, in fact, the poorest system investigated at all altitudes below 15,000 km.

Figure 39 illustrates the corresponding variation in power requirements for each of the above propulsion options. These variations with orbit altitude are substantially less severe than the IMIEO data of Figure 38.

These data would seem to imply, therefore, that the optimum Mars propulsion profile should involve the use of high thrust chemical propulsion from parabolic approach to a circular orbit at an altitude of 20,000 km and low thrust solar-electric propulsion after MEM rendezvous at the 20,000 km orbit to parabolic departure. However, this conclusion must be heavily qualified. The parabolic approach and departure velocity limitation on the investigation is an artificial limit which has been imposed as a result of a lack of data on low thrust heliocentric propulsion requirements with hyperbolic excess velocities at Mars. At Earth departure, when this limitation was not imposed, the optimum switching point was generally in the region of 5 km/sec hyperbolic excess velocity. It can be qualitatively argued that with optimized approach and departure velocities the advantage of the high thrust option should increase, and may lead to a low optimum altitude rather than a high one. These speculations can only be resolved by substantial additional investigations, as planned in follow-on to this study.

9.3 COMPARISON WITH ALL-HIGH-THRUST SYSTEMS

A preliminary study has been conducted to compare the hybrid nuclear rocket-nuclear electric vehicle performance characteristics with those of all-high-thrust chemical and nuclear rocket vehicles. The high thrust data has been taken directly from the work of General Dynamics/Convair.* The payloads used in these high thrust studies were substantially higher than those used in the current study; addtional nuclear-electric performance data was, therefore, developed using comparable payload characteristics in order to facilitate a direct comparison. Figure 40 summarizes the

*"Manned Mars and Venus Exploration Study" General Dynamics/Convair, Report No. GD/C A0K65-002-2, 21 May, 1965

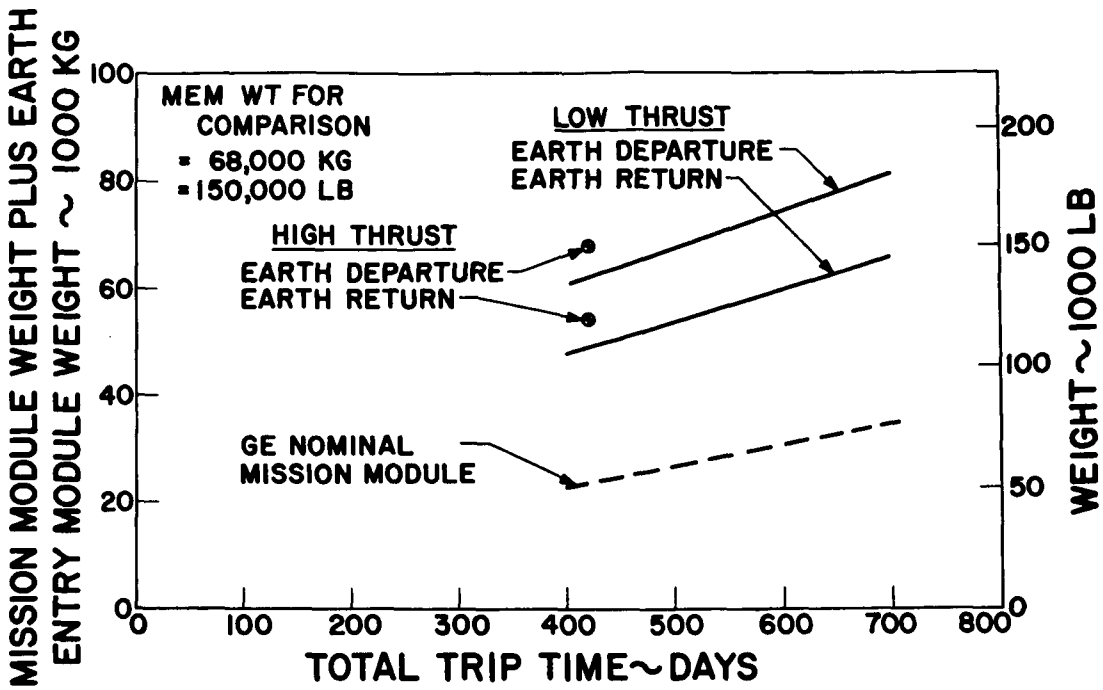

Figure 40. Payloads for Propulsion System Comparisons

reference high thrust payload characteristics and the comparable low thrust payload characteristics derived from the GD/C report. The differences between the high thrust payloads and the low thrust payloads at 420 days trip time are due primarily to the high thrust requirement for a separate mission module power supply, and secondarily to structural items which are accounted for elsewhere in the nuclear-electric vehicle.

The nominal GE payloads taken from Figure 4 have been included in Figure 40 for comparative purposes. It is noted that the high thrust payloads were based upon an early state-of-the-art semi-open life support system chosen on a cost-effectiveness basis for that mission. Low thrust vehicles have inherently longer trip times and, consequently, the nominal GE payloads reflect the choice of a more nearly closed life support system and a more reliable data handling system with fewer spare parts requirements.

Figure 41 presents the first results of the comparison study of the performance characteristics of chemical, nuclear-rocket, and hybrid nuclear rocket-nuclear electric propulsion for the manned Mars mission. This data is for a 1981-82 departure and a hyperbolic velocity earth return mode of operation. Chemical and nuclear rocket performance is shown for an optimum round trip time of 420 days for an opposition class mission. Although substantially reduced IMIEO requirements can be obtained for conjunction class missions with trip times of 900 to 1000 days, these data represent a sharp optimum of high thrust performance over the range of 400 to 800 days. Nuclear-electric performance, however, improves continuously as the trip time is increased over this range. At 420 days, the nuclear-electric performance at a powerplant specific weight of 15 kg/kw is substantially better than chemical and essentially the same as the nuclear rocket. At 520 days trip time, however, the nuclear electric IMIEO requirements are less than half of the optimum nuclear rocket requirements.

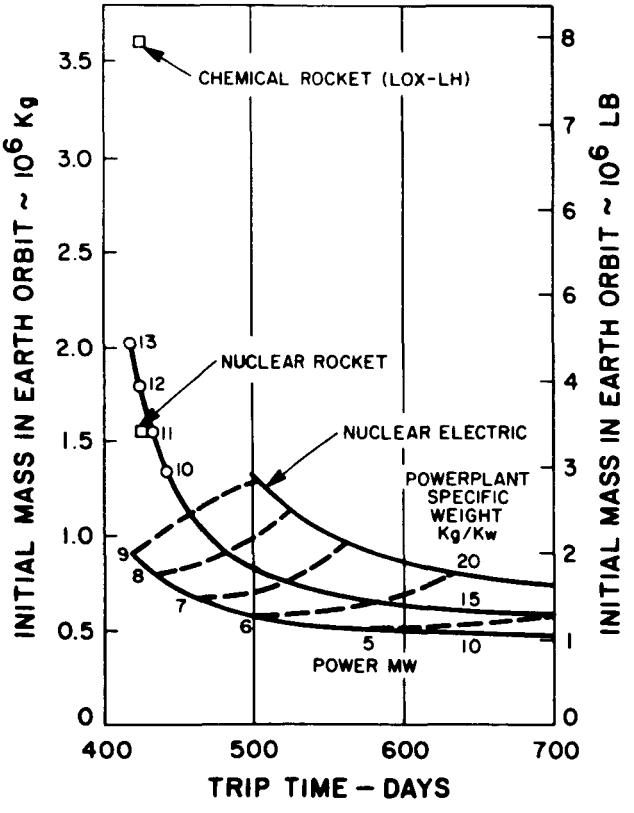

Figure 41. Propulsion System Comparison: 1981-82 Earth Departure, Hyperbolic Earth Return

As discussed in Section 5, the 15 kg/kw figure is essentially the current estimate of reasonably achievable performance for a dual powerplant Rankine cycle vehicle similar to the one discussed in Section 7.2. However, should reliability and orbit assembly considerations permit the use of a single powerplant, single reactor, vehicle, the powerplant specific weight can be reduced, at the same technology level, to 10 kg/kw. This would result in a vehicle weight (IMIEO) about half that of the nuclear rocket vehicle at the same 420 day trip time, and 1/3 of the nuclear rocket vehicle weight at a trip time of 520 days.

Figure 42 contains a similar performance comparison between chemical, nuclear-rocket, and nuclear-electric propulsion to illustrate the effects of launch year on system requirements. The chemical and nuclear-rocket data are based upon optimum round trip times which lie in the region of 420 to 460 days. The nuclear-electric data have been based upon operation at a powerplant specific weight of 15 kg/kw and on a trip time of 600 days. The most significant aspects of this comparison include the seven year shift in the best launch year between the high thrust and low thrust missions and the substantially reduced variation in IMIEO requirements over the complete synodic cycle for the nuclear-electric systems.

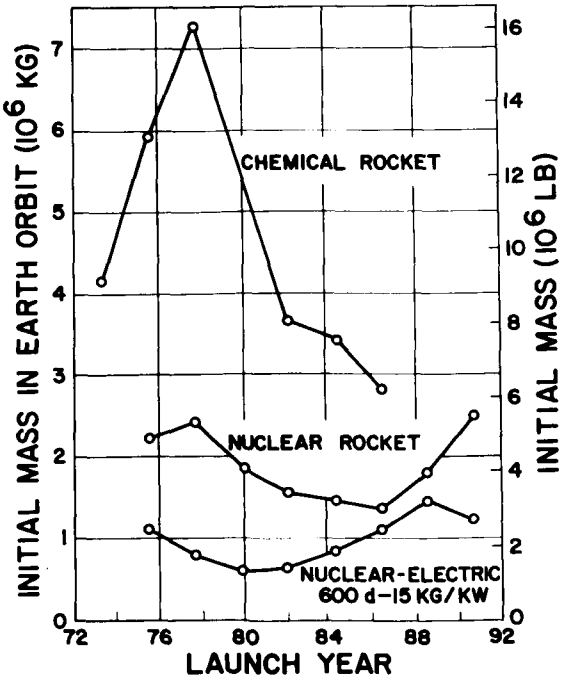

Figure 42. Launch Year Effect on IMIEO

I

SECTION 10

CONCLUSIONS

The conclusions drawn from the work to date have been collected in this section for the reader's convenience.. They are as follows:

1. The mission module weight ranges from 20 to 40 tons depending primarily on crew size and trip time, and secondarily on solar flare and meteorite models.

2. The Mars excursion module weight ranges from 30 to 100 tons depending on crew size and spaceship orbit altitude.

3. The performance and weights of present research ion thrustors and power conditioning components are adequate for the manned Mars mission, but improved performance and/or reduced weight would significantly improve the overall vehicle performance. The main requirement is for long time flight tests to demonstrate adequate life and reliability for both the thrustors and the power conditioning system.

4. The integration of ion thrustors into a multi-megawatt propulsion system results (in most cases) in an effective thrustor specific weight increase of 50 to 100% over the individual bare thrustor weight, due to support structure and redundancy requirements.

5. A nuclear Rankine cycle powerplant based upon a 5% fuel burnup, a 1284^{o}K (1850^{o}F) turbine inlet temperature, and a beryllium/stainless steel radiator would have a specific weight of 10 to 16 kg/kw depending on operating life, launch packaging constraints, and the choice between a single or a dual powerplant vehicle configuration.

6. Reliability factors require the use of all of the standard approaches (modularized powerplant and propulsion system designs, the selective provision of redundancy or reserve capacity, and an in-flight maintenance and repair capability) as well as a nominal mission plan based upon a declining power profile and a provision for abort-extended trip times. With these provisions, it appears that satisfactory reliability can be achieved without requiring outlandishly high component reliabilities.

7. A hybrid nuclear rocket and nuclear electric vehicle using the above thrustor and powerplant technology offers up to a factor of 2 reduction in initial mass in Earth orbit over that of an equivalent all-nuclear-rocket vehicle at the same trip time, and up to a factor of 3 reduction with a 25 to 40% increase in trip time.

8. It is technically possible to build, launch and deploy a multi-megawatt solar array (using 8 mil silicon cells) with an overall specific weight of 12 to 20 kg/kw. Such an array could be used as part of a manned Mars vehicle if a suitable dynamic environment can be insured. A major design study is needed to define the "suitable dynamic environment" as a function of the vehicle and array design characteristics.

9. Solar-electric vehicle performance can be only very roughly estimated until a firmer vehicle design emerges. Present estimates indicate that, with the 8 mil cells, performance with an optimum combination of high and low thrust may be competitive with other propulsion schemes. The availability of more advanced cells coupled with a favorable resolution of the dynamics question could lead to a performance advantage for solar electric.

10. The initial gross weight of a Low Acceleration Space Transportation vehicle is expected to fall between 500 and 1500 tons, depending mostly on crew size and trip time. At a given crew size and trip time, the weight can vary up to 50% due to the other factors mentioned above. This band of uncertainty can be markedly narrowed during the coming year through studies of the following areas:

    a) required crew operations (scientific, navigation, housekeeping, and maintenance and repair) as this affects crew size and vehicle reliability.

    b) Mars excursion module design, including the effects of varying crew size and orbit altitude.

    c) reactor assembly failure modes and effects as they influence the choice between single and dual powerplants.

    d) solar electric vehicle dynamics (structural response to normal control operations and to reasonable disturbances due to imbalance or misalignment) and the resultant strength (hence weight) required in the solar array.

    e) integration and optimization of high thrust units for use at Mars arrival and departure, including both nuclear electric and solar electric vehicles and both chemical nuclear rocket units for high thrust.

11. The development schedule and cost implied by the various vehicle concepts obviously require definition (along with definition of the required ground and orbital assembly and checkout operations) before an overall assessment of the attractiveness of the idea can be made. Our knowledge is now sufficient to permit a first cut at this task for the nuclear vehicle, and completion of the studies under 9 above should set the stage for this task for the solar vehicle.

12. The choice of the overall approach to manned interplanetary flight and, in fact, the decision to proceed with major system development both could be made on much firmer ground with the following in hand:

    a) better definition of the meteorite and solar flare environment and its effects on the crew and the vehicle systems.

    b) long time flight experience with crews of 6 to 12 men in space, with electric propulsion systems in space, and with a large nuclear reactor powerplant in space.